

1 Flow pattern evolution of the last British Ice Sheet

2

3 Anna L.C. Hughes ^{*1}, Chris D. Clark², Colm J. Jordan³

4

5 *Corresponding author.

6 ¹Department of Earth Science, University of Bergen, N-5007 Bergen, Norway; anna.hughes@geo.uib.no

7 ²Department of Geography, University of Sheffield, Sheffield, S10 2TN, UK; c.clark@sheffield.ac.uk

8 ³British Geological Survey, Keyworth, Nottingham, NG12 5GG, UK; cjj@bgs.ac.uk

9

10

11 Abstract

12

13 We present a 10-stage reconstruction of the evolution in ice-flow patterns of the last British Ice
14 Sheet from build-up to demise derived from geomorphological evidence. 100 flowsets identified in
15 the subglacial bedform record (drumlins, mega-scale glacial lineations, and ribbed moraine) are
16 combined with ancillary evidence (erratic-transport paths, absolute dates and a semi-independently
17 reconstructed retreat pattern) to define flow patterns, ice divides and ice-sheet margins during build-
18 up, maximum glaciation and retreat. Overprinting and cross-cutting of landform assemblages are
19 used to define the relative chronology of flow patterns and a tentative absolute chronology is
20 presented based on a collation of available dates for ice advance and retreat. The ice-flow
21 configuration of the last British Ice Sheet was not static. Some ice divides were remarkably stable,
22 persisting through multiple stages of the ice-sheet evolution, whereas others were transient features
23 existing for a short time and/or shifting in position 10s km. The 10 reconstructed stages of ice-sheet
24 geometry capture two main modes of operation; first as an integrated ice sheet with a broadly N-S
25 orientated ice divide, and second as a multi-domed ice sheet orientated parallel with the shelf edge.
26 A thick integrated ice sheet developed as ice expanded out of source areas in Scotland to envelop
27 southerly ice caps in northern England and Wales, and connect with the Irish Ice Sheet to the west
28 and the Scandinavian Ice Sheet across the North Sea. Following break-up of ice over the North Sea,
29 ice streaming probably drove mass loss and ice-sheet thinning to create a more complex divide
30 structure, where ice-flow patterns were largely controlled by the form of the underlying topography.
31 Ice surface lowering occurred before separation of, and retreat to, multiple ice centres centred over
32 high ground. We consider this 10-stage reconstruction of the evolution in ice-sheet configuration to
33 be the simplest palaeo-glaciological interpretation of the flowsets identified from the
34 geomorphological record and their relative timing. This empirically-based reconstruction of flow-
35 pattern geometry provides a framework for more detailed local and regional studies and numerical
36 modelling to provide robust explanations of the observed changes in ice-sheet structure in terms of
37 climate and glacial dynamics. As a minimum, numerical model outputs should be able to reproduce
38 the identified flowset patterns in space and satisfy their chronological order.

39

40

41 1. Introduction

42

43 Ice-sheet reconstruction aims to determine the past size, form and evolution of palaeo-ice sheets in
44 order to give time-constrained estimates of former ice-sheet volume, extent and form, and advance

45 and retreat rates. Such information is critical to improve and constrain ice-sheet modelling efforts
46 and understanding of ice-sheet behaviour over long timescales. Deciphering the evolution in ice-
47 sheet geometry as determined by the ice-flow pattern configuration is central to this endeavour.
48 Evidence-based reconstructions of flow-pattern dynamics locate the fastest (ice streams) and
49 identify the highest (ice divides) parts of the ice sheet, and how these changed over time. Using
50 such empirical reconstructions we can derive estimates of ice-sheet thickness and identify the
51 location and timing of ice-stream operation and thus likely calving fronts, which can be compared
52 with climatic and ocean changes during the last glaciation. Empirical reconstructions are also a test
53 for numerical ice sheet models (e.g. Hubbard *et al.*, 2009) that attempt to explain the controlling
54 glacial and climatic dynamics. Located on the edge of the North Atlantic and at the fringes of the
55 Eurasian Ice Sheet complex the last British Ice Sheet (BIS) and its counterpart the Irish Ice Sheet
56 potentially have a great deal to reveal concerning ice sheet-ocean-climate interactions. Even at its
57 largest extent, the combined British-Irish Ice Sheet was relatively small (comprising ~2.5 m Sea
58 Level Equivalent, Clark *et al.*, 2012) with a predominantly marine-based margin but was connected
59 at times to the larger Scandinavian Ice Sheet across the North Sea (Graham *et al.* 2007; Sejrup *et al.*
60 1994). The ice-rafted debris (IRD) record from the surrounding continental shelf is indicative of
61 persistent instability and continual readjustment of the ice sheet (e.g. Peck *et al.*, 2006), which has
62 also been indicated by numerical modelling (Hubbard *et al.*, 2009).

63
64 The general structure of ice-flow patterns across the British Isles was first synthesised from
65 recorded striations, inferred erratic transport paths, till lithological properties and mapped
66 streamlined-bedrock features at the turn of the twentieth century (Geikie, 1894; Wright, 1914,
67 Charlesworth, 1957) (Fig. 1a). Since, there have been few attempts to reconstruct ice-flow patterns
68 at the national or ice-sheet scale. Superimposed, cross-cutting drumlin patterns and variable size
69 distributions are exhibited by many of Britain's drumlin fields indicative of changes in the
70 configuration of the ice sheet and subglacial processes and/or environments (Rose and Letzer, 1977;
71 Letzer, 1987; Mitchell, 1994, 2007; Livingstone *et al.* 2008; Hughes *et al.* 2010). Several recent
72 local-regional scale reconstructions have provided tantalising glimpses into the ice-sheet evolution
73 noting considerable complexity and variation in time for discrete sectors of the BIS (e.g. Mitchell,
74 1994; Salt and Evans, 2005; Jansson and Glasser, 2004; Bradwell *et al.*, 2008a; Finlayson *et al.*
75 2010, 2014; Livingstone *et al.* 2010a, 2012). These studies demonstrate that individual ice divides
76 of the last BIS were spatially and temporally variable, and that their dominance varied over time.

77
78 In this paper we use countrywide mapping of the terrestrial subglacial bedform record (Hughes *et*
79 *al.* 2010; Hughes, 2009) supplemented with evidence from the marine record (e.g. Stoker and
80 Bradwell, 2005; Bradwell *et al.* 2007, 2008a; Graham *et al.* 2007, 2010; Stoker *et al.* 2009; Howe *et*
81 *al.* 2012) to synthesise flow-pattern information across the former ice-sheet bed and reconstruct the
82 ice-sheet scale flow-pattern evolution of the last BIS in its entirety. We focus on the British record,
83 but will necessarily make reference to the Irish Ice Sheet, and implications for the combined
84 British-Irish Ice Sheet. We build on the pattern of ice-sheet margin-retreat reconstructed by Clark *et*
85 *al.* (2012) by extending the reconstruction to include changes to the internal ice-sheet flow-pattern
86 geometry, both during retreat and the more challenging ice-sheet build-up phases.

87
88

89 2. Approach: palaeoglacial inversion

90
91 We rely on our interpretation of the landform record in terms of ice-flow vectors (*flowsets*),
92 augmented with data from the published literature, to produce a reconstruction via a logical
93 methodology and set of interpretative assumptions (e.g. Kleman *et al.* 2006; Greenwood and Clark,
94 2009ab). The reconstruction is principally geomorphological and we aim to produce the simplest
95 model that best explains most of the evidence and captures the characteristics of the ice sheet as a
96 whole. As with a reconstruction produced by numerical modelling, the final result may conflict with
97 some of the field evidence and serves to highlight sites and topics for further investigation. The
98 theoretical basis for this approach has been outlined in a series of preceding papers (Kleman and
99 Borgström, 1996; Kleman *et al.* 1997; Clark, 1997; Clark *et al.* 2000; Clark and Meehan, 2001; De
100 Angelis and Kleman, 2005, 2007; Kleman *et al.* 2006; Greenwood and Clark 2009ab; Trommelen *et*
101 *al.* 2012).

102 103 2.1 Glacial Maps

104 Our starting point is a comprehensive map of glacial landforms covering the terrestrial part of the
105 former ice-sheet bed (Hughes *et al.* 2010). We use what we believe is a near-complete map of the
106 subglacial bedform record of Britain (including drumlins, Mega-Scale Glacial Lineations (MSGSL),
107 crag and tails and ribbed moraine), produced by systematic remote mapping of the whole onshore
108 glaciated area from a high-resolution digital surface model (NextMap Britain DSM; 5 m horizontal
109 resolution) as the basis for the reconstruction of flow patterns. Break-of-slope digital capture of
110 each landform was conducted at a scale of 1:10000 or less. Full details of the mapping process
111 including quality control procedures are given in Hughes *et al.* (2010). Maps of moraine, esker,
112 meltwater channel and streamlined bedrock distributions derived from the same DSM source
113 (Hughes, 2009; Benn and Evans, 2010, Fig. 12.96; Clark *et al.* 2012, Figs. 4,5,7,8) and published
114 records of inferred erratic-transport paths as collated in the BRITICE database (Clark *et al.* 2004)
115 are integrated to inform flowset interpretation (Section 2.2.2) and provide independent geometric
116 information (Fig. 4). To our knowledge a comprehensive map of striations (e.g. Smith and Knight,
117 2011) has not been compiled for Britain, and we do not make reference to recorded instances of
118 striations. In mainland Britain striations tend to record local-regional flow patterns conforming to
119 undulations in the local topography (Evans *et al.* 2005) rather than the large-scale ice-flow
120 geometry, which is the focus of this work.

121 122 2.2 Flowsets

123 2.2.1 Flowset building

124 The first interpretative stage of the inversion approach is a process of rationalisation which reduces
125 the multifarious record contained within the glacial map into a manageable volume of information
126 by grouping landforms into summary assemblages or *flowsets*. *Flowsets* are identified by inspection
127 of the spatial arrangement of landforms with consideration of their morphometry, i.e. length,
128 elongation ratio (length/width), parallel conformity, spacing, and orientation (Fig. 2) (Greenwood
129 and Clark, 2009a).

130
131 We focus on the lineation record where each *flowset* defines a coherent group of drumlins, crag and
132 tails and/or MSGSL representing a discrete phase of ice flow (e.g. Boulton and Clark, 1990; Kleman

133 and Borgström, 1996; Clark, 1997; Kleman *et al.* 1997; Clark, 1999; Clark *et al.* 2000; Clark and
134 Meehan, 2001; DeAngelis and Kleman, 2007; Greenwood and Clark, 2009a). Instances of ribbed
135 moraine are relatively rare in Britain (Hughes *et al.* 2010), and ribbed moraine assemblages are
136 interpreted simply as ridges formed perpendicular to ice flow (e.g. Greenwood and Clark, 2009a)
137 rather than indicative of specific bed conditions (e.g. Trommelen *et al.* 2012; Dunlop *et al.* 2008).

138
139 Each flowset is classified in terms of the glaciological and temporal context of formation.
140 Classification is informed by bedform properties and spatial arrangements together with other
141 landform associations, e.g. with eskers and/or meltwater channels, using templates grounded in
142 theoretical concepts of landform generation (Table 1) (Kleman and Borgström, 1996; Clark, 1999;
143 Clark *et al.* 2000; Kleman *et al.* 2006; Greenwood and Clark, 2009a; Stokes and Clark, 1999). The
144 primary distinction is between *isochronous* flowsets that represent a single flow event at a point in
145 time (but which may have lasted for some time under a stable ice-sheet geometry) and smudged or
146 *time-transgressive* (TT) imprints produced by two or more flow events which are too subtly
147 different to be clearly separated. Flowsets were organised into a relative age stack by careful
148 examination of superimposition relationships of the constituent bedforms (Table 2) using the high-
149 resolution (5 m) digital elevation model used for mapping.

150

151 **2.3 Reconstruction process**

152 *2.3.1 Reconstruction ingredients*

153 The lineation flowsets and relative age order are the primary pieces of evidence used in the
154 reconstruction presented (Fig. 3, Tables 2 and S1). Generalised summaries of erratic transport paths
155 contained within the BRITICE database (Clark *et al.* 2004) and mapping of streamlined bedrock
156 (Hughes, 2009) are used as further support for and to supplement reconstructed ice-sheet flow
157 patterns (Fig. 5b). Streamlined bedrock and erratic distribution are regarded as second order
158 indicators of ice-flow patterns as they are likely to be the result of multiple ice-flow events, and
159 possibly the cumulative effect of several cycles of ice-sheet growth and retreat and no
160 interpretations are based on these indicators alone. As our glacial mapping is limited to the present-
161 day coastal boundary (Hughes *et al.* 2010; Hughes, 2009), we use published offshore evidence to
162 aid our reconstruction beyond the coastline. Where available, this includes moraines (e.g. Bradwell
163 *et al.* 2008a; Clark *et al.* 2012) and subglacial landforms (e.g. Graham *et al.* 2007, 2009; van
164 Landeghem *et al.* 2009). We use the retreat pattern of the last British-Irish Ice Sheet (Clark *et al.*
165 2012), reconstructed from maps of ice-marginal features (moraines, eskers, meltwater channels, and
166 glaciofluvial deposits) and flowsets classified as TT retreat type (n = 32) to define margin positions
167 during deglaciation and to tease out additional flowsets that were formed during retreat (Section
168 2.3.3, Fig. 5a). Timing of events is based on a database of published absolute chronological
169 information for the build-up and deglaciation of the last British-Irish Ice Sheet (Hughes *et al.* 2011)
170 which has already been used to date the pattern of marginal retreat (27-15 ka, Clark *et al.* 2012). We
171 use an updated version of the database with a census date of 1 May 2012
172 (http://www.sheffield.ac.uk/geography/staff/clark_chris/britice-chrono) (Fig. 5c).

173

174 *2.3.2 Inversion rules*

175 The interpretative process of inversion is subjective and different researchers may generate slightly
176 different interpretations from the same evidence. For this reason we outline the interpretative stages

177 involved and we make the subglacial bedform map (Hughes *et al.* 2010) and flowsets available for
178 scrutiny (Figs. 3, S1; Table S1). The following rules or assumptions inform our organisation of
179 flowsets into scenarios of ice-sheet geometry, and direct the choice of alternative scenarios where
180 they arise (after Greenwood and Clark 2009b).

- 181 1. *Symmetry*. Ice sheet geometry will be similar to modern ice sheets, i.e. tend towards a broadly
182 symmetrical plan form, with ice flow radiating out from divide locations, and comprising at
183 least one principle ice divide with the possibility of subsidiary divides branching off from the
184 main divide. Saddles will occur between connected divides.
- 185 2. *False divides*. Regions beneath divides are zones of landscape preservation. Divides must
186 therefore be upstream of a landform imprint and we must invoke divide migration when flow
187 patterns diverge in close proximity.
- 188 3. *Multi-temporal record*. We must invoke changes in configuration where more than one imprint
189 is superimposed and obey the relative chronology as defined by superimposition/stratigraphic
190 relationships.
- 191 4. *Extent*. Ice is not constrained to the present day terrestrial landmass. Ice is allowed to extend out
192 to the continental shelf in the North and West, to the Scilly Isles in the southwest, and the
193 southern drift limit in England when indicated by flow patterns.
- 194 5. *Avoid preconceived ideas*. Allow the reconstruction to develop as the evidence dictates.
- 195 6. *Minimum complexity*. Use the minimum number of divides to satisfy data. Attempt the simplest
196 solution, only conflicting evidence leads to a new configuration.
- 197 7. *Ice streams* are likely to have existed, and been integral to the ice sheet geometry (Bennett,
198 2003). They are presumed capable of driving rapid configuration changes. They may also briefly
199 cause asymmetric ice sheet form.

200

201 2.3.3 Reconstruction Process

202 The preserved record is fragmentary and incomplete by nature and so a degree of interpolation is
203 required to reconstruct plausible overall geometries from the identified flowsets. Potential flowset
204 groupings are assessed and rejected/accepted on the basis of spatial conformability and adherence to
205 the above rules (Section 2.3.2). The temporal component of flowset generation (isochronous or
206 time-transgressive) must also be satisfied. The process is iterative, and proceeds by continual
207 reassessment and modification as decisions are made and checked against the rules and
208 glaciological plausibility. Where it is not possible to determine the relative-age relationships
209 between flowsets a greater number of permutations can occur. In Britain, highly variable
210 topography over short distances means that there are many small discrete flowsets that do not
211 overlap (Fig. 3), and therefore had no relative age control (Table 2). This necessitated additional
212 and new approaches to reduce complexity and explore possible configuration geometries to reduce
213 the potential number of permissible permutations and connect fragmented records together (e.g.
214 Trommelen *et al.* 2012). Here, a regional approach was undertaken in the first instance where
215 relative age constraints were good (e.g. Figs. 5, 6), followed by analysis to distil the larger structural
216 elements of the ice-sheet-scale form to tie phases of the regional reconstructions together. Figs. 5
217 and 6 show the regional scenarios for NE England and northern Scotland as illustrative examples
218 and to show in more detail the interpretative decisions behind our final reconstruction (Section 3.2;
219 Fig. 8).

220

221 To identify tie-points that could be used to integrate the spatially disparate regional sequences of
222 information into plausible ice sheet scale geometries, we considered: i) the relationship between
223 topography and flowset size, ii) the location and size of ice stream signatures, and iii) coherence
224 with the retreat pattern derived from marginal landforms and TT retreat flowsets (Clark *et al.* 2012;
225 Fig. 7). This analysis created a synthesis framework from which we could tease out those flow
226 patterns from each region belonging to similar phases of the ice sheet history and link the regional
227 scenarios together. An inversion model of the neighbouring Irish Ice Sheet (Greenwood and Clark,
228 2009b) was used as a final extra check to decide between alternative scenarios.

229
230 We interpret flowsets that disregard topography as a record of the *pre-deglacial* ice sheet
231 configurations and as providing a glimpse of ice-sheet geometry during maximum extent. We
232 assume that these *pre-deglacial* flowsets (where there is no contradictory evidence and the resultant
233 configuration appears plausible) to belong to broadly the same ice-sheet configurations and act as
234 tie-points for combining the regional reconstruction sequences. The majority of the remaining
235 flowsets (where there is no contradictory evidence and the resultant configuration appears plausible)
236 are regarded as documenting the changing geometry of the ice sheet during deglaciation. This
237 interpretation is supported by the fact that flowsets that disregard topography are generally the
238 oldest in the relative age stack (Table 2) and most of the remaining flowsets are consistent with the
239 reconstructed pattern of retreat (Fig. 7).

240
241 The retreat pattern is dependent, in part, on the organisation of the ice-sheet geometry immediately
242 prior to and during retreat. The retreat pattern over Britain has been previously reconstructed from
243 the distribution of moraines, meltwater channels, eskers, glaciolacustrine sediments and a fraction
244 of the flowsets; those identified as formed behind a retreating ice margin (Table 1: TT retreat type,
245 Table S1: n = 32, Clark *et al.* 2012). The TT retreat flowsets are by definition part of the deglacial
246 signature. The remaining 68 flowsets were not used in the retreat pattern reconstruction of Clark *et al.*
247 (2012), as internal ice-flow patterns and ice-divide locations were not reconstructed as part of
248 that work for Britain. The retreat pattern therefore provides a valuable guideline to identify which
249 flowsets, in addition to those of TT retreat type, were formed during deglaciation and as a check on
250 our assumption that most topographically-controlled flowsets that are preserved are associated with
251 deglacial stages.

252 253 254 **3. Flow patterns and evolution of the last British Ice Sheet**

255 256 **3.1 Flowsets of the last British Ice Sheet (Fig. 3, Fig. S1, Table S1)**

257 We identify 100 lineation flowsets in the British subglacial-landform record (Fig. 3; Table S1).
258 Approximately one third of the flowsets are classified as isochronous (n = 37). Smudged (time-
259 transgressive) imprints are not restricted to deglacial flow events (e.g. Clark *et al.* 2000); 32 are
260 interpreted to have formed behind a retreating ice margin (TT retreat), 14 record
261 increasing/decreasing effect of topography (TT thinning/thickening) and 8 are interpreted as the
262 result of a shift in the ice divide location (TT flowline). 10 flowsets exhibit characteristics of ice
263 streams. We have confidence in 85 flowset classifications. There are 15 flowsets, (generally those

264 composed of only a handful of landforms or within highly complex zones) that cannot be classified
265 (Table S1).

266

267 Flowsets with topographic congruence are generally the youngest in the relative age stack and
268 collectively require multiple ice-divide locations over most areas of high ground (Fig. 7b; Tables 2;
269 S1). Flowsets that disregard topography are located roughly east and west of an imaginary line
270 running approximately north-south, require ice centres on both high and low ground and are
271 generally the oldest in the relative age stack (Fig 7a, Tables 2; S1). In addition to the 32 TT retreat
272 type flowsets, 28 flowsets of isochronous, TT flowline and TT thinning/thickening type document
273 flow patterns that conform to the reconstructed pattern of retreat and therefore are likely
274 representative of the changing ice-flow geometry during deglaciation (Fig. 7c).

275

276 Ice streams have been identified or postulated in The Minch (Stoker and Bradwell, 2005), Witch
277 Ground (Graham *et al.* 2007), Strathmore (Golledge and Stoker, 2006), Tweed (Everest *et al.* 2005),
278 Tyne Gap (Livingstone *et al.* 2010a; Evans *et al.* 2009), eastern England (North Sea Lobe, Evans
279 and Thompson, 2010; Boston *et al.* 2010, Davies *et al.* 2012; Roberts *et al.* 2013), Irish Sea (Evans
280 and Ó Cofaigh, 2003; Roberts *et al.* 2007), North Channel (Greenwood and Clark, 2009b) and the
281 Hebrides (Howe *et al.* 2012), Moray Firth (Merritt *et al.* 1995) and Firth of Forth (Fig. 7d). We
282 identify signatures of most of the terrestrially-based ice streams in our flowsets (Table S1; *fs4*, *fs5*,
283 *fs6*, *fs8*, *fs10*, *fs11*, *fs18*, *fs19*, *fs51*, *fs56*, *fs99*). On the basis of size and relative chronology it is
284 possible to organise our ice-stream flowsets into groups representing at least two possible ice-flow
285 configuration frameworks. One grouping (Minch-*fs4*, Strathmore 1-*fs51*, North Channel -*fs8*, Irish
286 Sea -*fs18*) is proposed to occur during maximum extent when the ice sheet was confluent with ice
287 in the North Sea and reached the continental shelf edge. During maximum stages ice streams occur
288 at the junctions between ice masses, e.g. Scottish and Irish ice in the North Channel and mainland
289 Scottish and Outer Hebrides ice in the Minch, and there must be an ice divide running broadly N-S
290 over Highland Scotland and a connection with the Irish Ice Sheet. *Fs51* (Strathmore 1) is tentatively
291 correlated with the Witch Ground Ice Stream (Graham *et al.* 2007). A second group of ice streams
292 (Tweed -*fs10*, Strathmore 2 -*fs56*, Moray Firth -*fs6*, Forth *fs19*, Tyne Gap *fs11*) are all restricted to
293 the onshore record, indicate topographic confinement, and suggest a more complex divide structure
294 However, within the second group not all flowsets can be associated with the same stage. In
295 compliance with the relative chronology we associate *fs10*, *fs56* and *fs6* with the later (deglacial)
296 and *fs19*, *fs11* with the earlier (build-up) phases of ice sheet evolution.

297

298 **3.2 Flow pattern evolution of the last British Ice Sheet**

299 Following the rules and process outlined in Section 2 we present the simplest glaciologically-
300 plausible explanation of the preserved geomorphological record (Fig 8, Table 3).

301 **3.2.1 Stage 1**

302 The oldest flowsets in Scotland are large and topographically unconstrained and therefore
303 necessitate a large ice cap centred on the Scottish Highlands (*fs7*, *fs33*, *fs2*; Tables 2 and 3).
304 Grouping these flowsets together requires a main ice divide running along the NW Highlands and a
305 secondary fork over the Grampian Mountains. Deflection of ice to north (*fs33*) and south (*fs7*) in the
306 west is explained by the position of this secondary divide. Evidence is all on the eastern side of the
307 ice sheet, the western side is inferred from rule of symmetry. East-west orientated ice flow over the

308 Western Highlands is consistent with the generalised orientation of streamlined bedrock (e.g.
309 Bradwell *et al.* 2008b) and erratic evidence (Clark *et al.* 2004) (Fig. 4b). A connection with an ice
310 cap centred on the Outer Hebrides is inferred from the absence of erratic evidence for overriding of
311 these islands by ice from mainland Scotland during the last glacial period. This necessitates
312 deflection of ice around the islands and supports the development in later stages of ice streams
313 along The Minch trough (Stoker and Bradwell, 2005) and south of the Hebrides (Howe *et al.* 2012).
314 The orientation of *fs2* suggests no connection with ice cover over Shetland at this time, and we
315 place the ice-sheet margin to the south of Orkney. Placement of the ice divide upstream of the flow
316 pattern inscribed by *fs2* and *fs7* necessitates that the south-western margin is placed over the North
317 Channel close to northern Irish coast by rule of symmetry. This stage occurs prior to (but sets up
318 conditions for) an incursion of Scottish-sourced ice into Northern Ireland, the earliest stage (Stage I)
319 reconstructed by Greenwood and Clark (2009b). It is possible that both the southern and northern
320 margins were more extensive, and that ice masses had started to develop on high ground to the
321 south and on Shetland but without adequate evidence to define their boundaries they are not marked
322 on the maps.

323 3.2.2 Stage 2

324 *Fs52* indicates ice flow from a source in western Scotland curving towards the east coast. We
325 interpret this deflection as due to a competing ice source centred on the south-western Southern
326 Uplands. South-westerly extrapolation of the northwest-southeast orientated ice flow of *fs52* from a
327 source over the western Highlands and Islands of Scotland moving over the Firth of Clyde explains
328 presence of shelly till in Ayrshire (Fig. 4b) and is consistent with the ice-flow direction inferred
329 from the large area of ribbed moraine in the region (*rm2*; Fig. 3 inset map). *Fs2* fits into Stages 2-4
330 suggesting relatively stable ice-flow directions in the northern sector, but we extend the northern
331 and western margins further out onto the shelf to mirror the southerly expansion. *Fs33* is classified
332 as TT flowline type and shows a minor shift in flow pattern orientation which we infer as due to
333 movement of the principal ice divide to the southwest, consistent with convergence with a Southern
334 Uplands ice mass. We depict incursion into Ireland but the geometry is also consistent with
335 connection to an Irish-sourced ice mass.

336 3.2.3 Stage 3

337 Deflection of ice around the Lake District and down the Vale of Eden to the east (*fs57*) indicates
338 further expansion of Scottish-sourced ice south and connection to a Lake District ice dome. We
339 infer development of the Southern Upland ice dome into a secondary divide and a shift of the
340 primary divide to the southeast. The connection between Highland and Southern Upland ice
341 becomes centred over low ground. The position of *fs8* implies an ice divide (or saddle) across the
342 North Channel and we propose this flowset represents the vestigial terrestrial imprint of an ice
343 stream draining the Irish and Scottish Ice Sheets towards the Barra Fan (North Channel Ice Stream)
344 as also reconstructed by Greenwood and Clark (2009b). Both the size of the Barra Fan, the
345 prominence of the bathymetric trough in the North Channel and sea-bed morphology lead us to
346 suspect that this was an important ice flow path for the last BIS and likely formed a substantial ice
347 stream network together with ice from Ireland (Barra Fan Ice Stream, Scourse *et al.* 2009; Dunlop
348 *et al.* 2010) and northern Scotland (Hebrides Ice Stream, Howe *et al.* 2012). We maintain the
349 secondary divide over northeast Scotland from the previous stage, which results in a shift to west-
350 east orientated ice flow over central-eastern Scotland. An ice stream may have developed in the
351 Moray Firth at this time, although we have no direct evidence for this. Although not depicted on

352 Fig. 8 an ice cap on the Welsh uplands is inferred from subsequent stages. This configuration
353 corresponds to Stage II in Ireland as reconstructed by Greenwood and Clark (2009b).

354 3.2.4 Stage 4

355 A major ice divide running broadly north-south from western Scotland to west of the Lake District
356 is inferred from evidence for major west-east ice flow across northern England and central Scotland
357 (*fs19, fs11, fs30*). Secondary divides over eastern Scotland follow from the preceding stages and the
358 orientation of flow-lines. We infer development of the Irish Sea Ice Stream and strengthening of the
359 North Channel Ice Stream as ice is forced around the Irish Ice Sheet. Ice streams discharge into the
360 North Sea (*fs19, fs11*). Both *fs19* and *fs11* are classified as TT thinning/thickening type, which we
361 interpret as due to an increase in ice-surface elevation relative to the bed topography during a period
362 of stable W-E ice flow. As in the preceding stage this configuration would permit an ice stream in
363 the Moray Firth, but no explicit flowset is associated with this. *Fs19* is splayed at the coast
364 suggesting termination at a terrestrial ice margin and therefore this stage is placed before any
365 connection with the Scandinavian Ice Sheet in the North Sea. Smudging within *fs2* indicates a slight
366 shift in flow patterns to a south-north orientation over northern Scotland. We infer connection with
367 a substantial Welsh ice cap by this stage with an ice divide running broadly north-south (*fs22*) as
368 there is no evidence for invasion of Wales by the Irish Sea Ice Stream as it advances south. This and
369 Stage 5 correspond to Irish Stage IIIa/b (Greenwood and Clark, 2009b).

370 3.2.5 Stage 5

371 Eastern flow patterns are diverted to the north (*fs34*) and south (*fs13*) and ice flow over Scotland
372 switches towards the north-northwest (*fs1*) consistent with striae and erratic evidence (Sissons,
373 1967, Fig. 39; Figs. 6 and 4b). Ice flow orientated SE-NW overwhelms Shetland (*fs59*). We invoke
374 confluence with the Scandinavian Ice Sheet over the western North Sea (Sejrup *et al.* 1994) to
375 explain these 90 degree shifts in ice flow across the east of the country and the first major change in
376 ice-flow patterns in northern Scotland (Fig. 6). Marine sediments found in Caithness at the tip of
377 northeast Scotland support ice flow moving onshore from the south (Sissons, 1967, Fig. 39; Figs. 6
378 and 4b). North-south orientated ice flow patterns over the North Sea are derived from the
379 orientation of MSGL attributed to the Witch Ground Ice Stream (Graham *et al.* 2007). These flow
380 pattern changes show that the primary ice divide shifted ~60 km south and switched from to a
381 north-northwest to south-southeast alignment. *Fs9* over southwest Scotland is included here as is
382 difficult to incorporate into other stages but could also be incorporated into Stage 4; *fs9* indicates a
383 ~50 km shift north of the connecting saddle/divide between Scotland and Ireland, consistent with
384 advancement and increasing catchment size of the Irish Sea Ice Stream and reorganisation of ice
385 flow over eastern Scotland. Growth of the Irish Sea Ice Stream catchment area reduces the
386 catchment area and probably results in a decline in vigour of the North Channel Ice Stream
387 (Greenwood and Clark, 2009b). A Welsh ice cap develops (*fs22*) and we extend the Irish Sea Ice
388 Stream to the south as its catchment area increases around the Welsh ice cap (*fs17*). The main ice
389 divide over northern England shifts east as the Irish Sea Ice Stream develops, which was probably
390 pinned against Pembrokeshire-Southern Ireland.

391 3.2.6 Stage 6

392 Ice flow over central-eastern Scotland switches to broadly west-east orientation (*fs51*). Deflection
393 of *fs51* to the north suggests maintenance of significant ice in the southern North Sea or a matching
394 southerly flowing (and possibly surging) ice lobe along northern English coast (North Sea Lobe;
395 Evans and Thompson, 2010; Boston *et al.* 2010) which would also be consistent in the preceding

396 and following stages. The principle ice divide is pushed west and north to accommodate *fs51* and
397 *fs18* and southerly orientated ice flow over northwest England (*fs31*) creating a new tripartite divide
398 structure . This requires a return to west-east ice flow over northeast England and eastern Scotland.
399 The secondary divide over eastern Scotland disappears and the centre of the ice sheet is shifted
400 south. Ice streams operate in Strathmore (*fs51*), Irish Sea (*fs18*), and The Minch (*fs4*) and the
401 documented advance of the Irish Sea Ice Stream to the Isles of Scilly (Scourse and Furze, 2001;
402 Hiemstra *et al.* 2006) is placed in this stage. We infer further concomitant decline of the North
403 Channel Ice Stream initiated in the preceding stage. We thus expand on the details of the
404 competition between these two central ice streams and the evolution of the North Channel saddle as
405 was inferred in Stage IV of Greenwood and Clark (2009b). From this stage onwards marginal
406 positions are based on the retreat-pattern reconstruction of Clark *et al.* (2012). Based on the
407 available chronological information (Section 3.3) we start retreat of ice from the shelf edge and in
408 the northern North Sea (Clark *et al.* 2012).

409 3.2.7 Stage 7 (*time-transgressive*)

410 East-west ice flow over northern Scotland (*fs3* and *fs62*) requires a resumption of an ice divide
411 located over the northwest Highlands. This ice divide is dominant over Grampian-sourced ice
412 although a western secondary divide can be accommodated and is re-established in full in the
413 following stage. An independent but connected ice cap on Shetland orientated northeast-southwest
414 is also inferred back from subsequent stages. The ice sheet margins are stepped back following the
415 retreat pattern reconstruction (Clark *et al.* 2012). Topographically constrained fast-flowing ice
416 flows west to east over northern England (*fs10*). At the coast ice flow is deflected southwards either
417 due to a remnant ice mass over the southern North Sea, or as part of a major ice tongue from
418 northern England, ‘North Sea Lobe’ (see Clark *et al.* 2012). *Fs69*, *fs99*, *fs18* and *fs84* show the
419 changing effect of ice flow patterns emanating into the eastern Irish Sea as the ice stream retreats,
420 and the thinning effect on the ice sheet in northern England (*fs20*, *fs10*). The Irish Sea deglaciates
421 rapidly (e.g. Chiverrell *et al.* 2013 and references therein), but likely punctuated by multiple
422 oscillations of the ice margin, as dictated by the retreat pattern reconstruction (Clark *et al.* 2012). As
423 parts of the ice sheet uncouple smaller ice masses expand once buttressing is removed. *Fs42*, *fs21*
424 and *fs16* describe initial retreat and decoupling from the Welsh ice cap. Stage 7 corresponds with
425 Irish Stage Va (Greenwood and Clark, 2009b).

426 3.2.8 Stage 8 (*time-transgressive*)

427 Retreat in northern England progresses by thinning (*fs48*) then retreat to local high ground, as
428 dictated by the retreat pattern, with accordant local changes in flow patterns (*fs70*, *fs71*, *fs41*, *fs80*,
429 *fs65*, *fs66*, *fs43*), the details of which are not shown on Fig. 8. The Lake District-Yorkshire Dales
430 centred ice mass separates from a now predominantly Scottish-centred ice sheet. Short lived local
431 oscillations of the ice sheet margins likely occur during separation of each ice mass. Progressive
432 thinning of the Scottish ice mass occurs (*fs5*, *fs56*, *fs45*), which remains reasonably extensive to
433 account for ice moving down the northeast coast, necessitated by the retreat pattern, and a
434 connection with Irish ice is maintained (*fs39*, *fs40*). The Scottish ice divide shifts west to return to
435 its Highland position possibly due to reactivation and retreat of The Minch Ice Stream (*fs5*). The
436 Welsh ice cap starts to retreat and thin, breaking into two separate domes (*fs76*, *fs74*, *fs87*, *fs91*).
437 Stage 8 corresponds with Irish Stage Vb-c (Greenwood and Clark, 2009b).

438 3.2.9 Stage 9 (*time-transgressive*)

439 Ice over northern England and Wales is reduced to small ice caps and glaciers. Separated from the
440 Irish Ice Sheet a saddle forms between separate Highland and Southern Upland centred ice divides
441 (*fs25, fs24*) as the ice sheet thins. We infer separation of a Shetland ice cap by shrinking of offshore
442 margins and symmetry (*fs61*). From the relative chronologies of the retreat pattern and flowsets ice
443 had retreated inland from the northeast Scottish coast and an ice lobe emanating from the Moray
444 Firth (*fs6*) flows onshore (*fs100*). A thin ice sheet is documented by network of small ice-stream
445 flowsets (*fs45, fs56, fs64, fs26, fs64*) deflected by topography in central and eastern Scotland. An
446 ice dome is inferred centred on the Cheviots (Clapperton *et al.* 1970) to account for deflection of ice
447 flow patterns around the area (*fs14, fs12* and *fs37*) and satisfy the retreat pattern. This stage
448 corresponds to Irish stage VI-VII (Greenwood and Clark, 2009b).

449 3.2.10 Stage 10 (time-transgressive)

450 Final retreat to Highland Scotland progresses by topographically constrained ice flow (*fs46, fs79,*
451 *fs44, fs55, fs53, fs47, fs82*). Minor expansion of Highland ice occurs following uncoupling from
452 Southern Upland ice mass to account for flow patterns *fs23* and *fs28*.

453
454 During the final time-transgressive stages (Stages 7-10) the snapshot nature of the reconstruction
455 misses any oscillations and readvances that occurred as the ice sheet separated into constituent
456 parts, which are not individually shown in the maps (e.g. ice-free enclaves identified in northern
457 England occurring before final retreat of ice from the Irish Sea and Lake District (Livingstone *et al.*
458 2010bc, 2012)). Only five flowsets could not be explained within these 10 stages and may be
459 inherited from a previous glaciation (*fs96, fs97, fs92, fs35* and *fs93*). Of these, all except *fs35*, are
460 based on fewer than 10 lineations and could not be classified (Table S1).

461

462 3.3 Timing of events

463 Our 10-stage reconstruction of the ice-sheet configuration respects the sequence of events described
464 by the relative-age relationships of the constituent flowsets (Table 2). At present there is no
465 satisfactory way to directly date palaeo-ice flow-lines and therefore we must consider the available
466 dates that 'bracket' advance and retreat of the ice sheet to add an absolute chronology (e.g. Kleman
467 *et al.* 2006). There are relatively few dates that constrain the timing of build-up of the ice sheet, and
468 no clear pattern emerges from the spatial distribution of the dates that do exist (Chiverrell and
469 Thomas, 2010; Hughes *et al.* 2011). This reflects multiple nucleation sites and the asynchronous
470 nature of the maximum limits in different sectors of the ice sheet (Clark *et al.* 2012) as well as
471 preservation issues for older dates. The youngest dates constraining ice build-up cluster ~30 ka BP
472 (Lawson, 1984; Sutherland, 1984; Sutherland *et al.*, 1984; Hedges *et al.*, 1994; Fitzpatrick, 1965;
473 Jardine *et al.* 1988; von Weymarn and Edwards, 1973; Sutherland and Walker, 1984). Marine core
474 evidence from the Barra Fan suggests that the ice sheet had marine margins by ~29 ka BP (Scourse
475 *et al.* 2009), and had expanded to the shelf edge in multiple locations by ~27 ka BP (Wilson *et al.*
476 2002; Everest *et al.* 2013). Together with our reconstruction of ice-flow pattern build-up (Stages 1-
477 3) this evidence suggests that the younger ages (as above) seem improbable and require revisiting
478 (see also Bradwell *et al.* 2008a). Although we correlate Stages 2 and 3 with Irish Stages I and II of
479 Greenwood and Clark (2009b), we suggest a slightly later timing based on the Scottish chronology;
480 Stages 1-3 occurring between 32-28 ka. We place Stages 4 and 5 as occurring ~28-26 ka. Confluent
481 ice cover over the North Sea must have occurred prior to 25 ka BP but after 33 ka BP (Sejrup *et al.*
482 1994), and European rivers discharged onto the Celtic continental margin via the English Channel

483 (Fleuve Manche) between 30-18 ka (Toucanne *et al.* 2010). The Irish Sea Ice Stream maximum
484 advance to the Isles of Scilly was likely a short lived event occurring ~24-23 ka BP (Ó Cofaigh and
485 Evans, 2007; McCarroll *et al.* 2010; Chiverrell *et al.* 2013) and so Stage 6 is placed at ~24 ka.
486 Stages 7-10 are placed as occurring ~22-15 ka following on from the reconstructed retreat pattern
487 (Clark *et al.* 2012); additional dates included in the updated database can be accommodated within
488 error bounds. Ice had retreated from the majority of northern England by 17 ka (Stage 9) (Pinson *et al.*
489 *et al.* 2013). High-elevation summits became exposed due to ice-sheet thinning at ~20-17 ka in Wales
490 (Glasser *et al.* 2012) and ~16-15 ka in NW Scotland (Fabel *et al.* 2012).

491

492 **4. Discussion**

493

494 Our model is consistent with many of the long-established ice-divide locations; Highland Scotland,
495 Southern Uplands, Grampians, Cheviots, Outer Hebrides, Shetland, Lake District, Pennines and
496 Wales (Evans *et al.* 2005 and references therein). During maximum extent the last BIS operated as
497 an integrated ice sheet, first with a primary N-S ice divide running along the western mountainous
498 regions from North Scotland to the southern Lake District (Fig 8; Stages 4-5), and then switching to
499 a shelf-edge parallel configuration with a primary divide running NE-SW across the North Channel
500 following confluence with the Scandinavian Ice Sheet (Fig 8; Stages 5-6). The flow pattern
501 configuration during confluence of British and Scandinavian ice is remarkably similar to that
502 produced by Geikie (1894). Flow pattern changes after ~22 ka document development of a
503 polycentric ice-sheet structure before disintegration to multiple locations, the youngest flow patterns
504 recording changes and oscillations as local ice centres re-establish and uncouple (Stages 7-10).
505 Initial growth of ice from Scotland (Stages 1-2), movement of the ice-sheet centre south (Stages 3-
506 6) and eventual emergence of an ice sheet characterised by multiple divide locations and far
507 travelled lobes (Stages 7-10) also compares favourably with recent numerical models of the ice-
508 sheet flow pattern evolution (Boulton and Hagdorn, 2006; Hubbard *et al.* 2009).

509

510 Our untangling of the sequence of events shows that the landform record provides glimpses of
511 build-up of the ice sheet. Ice expands out of Highland Scotland into Ireland uninhibited by Irish ice,
512 suggesting that the Irish Ice Sheet was not substantial enough at this stage to deflect Scottish ice
513 (Greenwood and Clark, 2009b). In contrast, deflection of ice around Wales and local ice caps over
514 Lewis, the western Southern Uplands and Lake District (Fig 8; Stages 2-4) implies that these ice
515 masses existed prior to advance of Highland-sourced ice. Whereas local ice caps over the Southern
516 Uplands and Lake District were subsumed into the main ice divide (Fig 8; Stage 4), the Welsh ice
517 cap remained an independent feature throughout (Fig 8). This is in agreement with the conclusion of
518 Jansson and Glasser (2008) but contrasts with the results of numerical modelling that show ice
519 expansion from a single Scottish ice mass invading both Ireland and Wales (Boulton and Hagdorn,
520 2006).

521

522 Some ice divides are persistent features recurring in successive flow geometries whilst others are
523 transient, and some experience substantial migrations (6-100 km). The most persistent feature is the
524 N-S 'Highland Scotland' ice divide, which shifts in absolute position (and extension south),
525 pivoting from N-S through NW-SE, NE-SW and returning to a N-S orientation, but remains a
526 characteristic feature of all time-slices (Fig 8). The near-constancy of this divide is reflected in the

527 dominant direction of glacial-erratic transport to the east or west either side of the approximate
528 location of this N-S trending divide (based on published erratic data compiled in Clark *et al.* 2004;
529 Fig. 4b). The Welsh ice divide is also a particularly stable feature moving <10 km to the east and
530 west, and once established the divide/saddle connection to the Irish Ice Sheet persists across the
531 North Channel (despite shifts of up to 40 km in absolute position) until the latest deglacial stages. In
532 northern England and southern Scotland ice-flow-pattern geometry is highly dynamic, (see also Salt
533 and Evans, 2005; Mitchell, 1994, 2007; Evans *et al.* 2009; Livingstone *et al.* 2008, 2010abc;
534 Finlayson *et al.* 2010, 2014) reflecting the change from the simpler maximum extent flow
535 configuration to one of multiple competing ice domes as deglaciation progresses. This result
536 explains the complex landform record and flowset overprinting found in this central sector of the
537 country (Fig 3; Hughes *et al.* 2010) and demonstrates that the landform record chronicles several
538 different ice-sheet configurations. Predominantly west-east ice-flow patterns initially record ice
539 flow breaching the Pennines from an ice divide centred on, or west of, the Cumbrian Mountains.
540 From this position the ice divide pivots eastward ~50 km to run WSW to ESE from the Cumbrian
541 Mountains to the Howgill Fells, demonstrating that an ice dome centred on the Lake District only
542 occurred during deglacial and early build-up stages.

543
544 A major revelation evident from the flowset map (Fig. 3) is the close relationship of ice-flow
545 patterns with topography in Britain. The majority of flowsets exhibit at least some accord with
546 topographic variations (Fig. 7b). Our examination of relationships between flowset types, sizes,
547 relative ages and geometries with the underlying topography and the retreat pattern lead us to
548 propose that topography had the greatest influence on flow patterns during deglaciation; thick ice
549 (relative to topography) was maintained until the maximum extent was reached (Stages 5-6) after
550 which ice-surface lowering preceded longitudinal retreat. Our logic is that flowsets that ignore
551 topographic variations were produced when the direction of ice-surface slope was dominant in
552 controlling ice-flow direction. Flowsets constrained by topography were generated when variations
553 in the subglacial relief were the dominant control. Under thick ice, the location and migration of
554 divides alone controls the evolution of flow-pattern configuration but as the ice thins the topography
555 of the bed increasingly influences flow-pattern geometry, eventually dominating over orientation
556 changes resulting from divide migration (Kleman and Hättestrand, 1999; Kleman *et al.*, 1999). The
557 last BIS is interpreted to have undergone such a transition, and we hypothesise that the change in
558 configuration occurred due to the presence or absence of marine-terminating margins (Fig. 9). At
559 maximum extent the ice extends to the edge of the continental shelf creating extensive marine-
560 terminating margins (Stages 4-5). When accumulation exceeds ice loss (by melting and calving) the
561 ice sheet grows yielding a thick ice sheet where divide location and flow geometry are largely
562 independent of topography (i.e. an ice sheet *sensu stricto*) (Stages 5-6). When ice loss exceeds
563 accumulation, the ice sheet thins and the flow geometry is increasingly influenced by basal
564 topography; ice divides becoming anchored to major upland areas (creating a complex of ice caps)
565 (Stages 7-9).

566
567 In support of this conceptual interpretation the retreat pattern also records a signature of ice-sheet
568 thinning (Clark *et al.* 2012). For example, lateral meltwater channels document lobes of ice
569 retreating around the topographic obstacle of the Forest of Bowland towards the Howgill Fells
570 (Hughes, 2009; Clark *et al.* 2012). This is consistent with the reconstructed flow-pattern evolution

571 which records a change from ice flow overriding the topographic bump (*fs31*; Stage 6) to being
572 deflected around it (*fs69, fs70, fs73*; Stage 7). The same sequence of early topographically-
573 unconstrained ice flow followed by ice flow along major valleys was also proposed for the Welsh
574 ice cap (Jansson and Glasser, 2004, Glasser *et al.* 2012). The later stages of the BIS appear more
575 analogous to the present day Antarctic Peninsula (Rignot *et al.* 2011) and later stages of the
576 Scandinavian (Arnold and Sharp, 2002) and Innuitan Ice Sheets (England *et al.* 2006). The ice sheet
577 therefore had different styles of operation; dynamics of mountain-centred or heavily
578 topographically-governed ice sheets are different to thick ice sheets, especially in the scale and
579 timing of response to climate. For example, ice flow will be funnelled to specific locations and
580 increasingly divided into fast and slow flow regimes over short distances with an increased potential
581 for a complex hydrological system, possibly creating an ice sheet more sensitive to external climatic
582 changes. Retreat rates are also likely to be spatially variable dependent on the specific topographical
583 setting of each section of the ice sheet margin (Jamieson *et al.* 2012).

584
585 The pattern of deflection followed by retreat around (rather than over or towards) topographic
586 obstacles is repeated around the country at various scales (Stages 7-10). For example, ice is
587 deflected by and retreats around the Cheviots (Fig. 5), Moray Firth and Strathmore ice lobes retreat
588 around the Eastern Grampians, the Irish Sea Ice Stream is deflected by and retreats around the
589 Welsh ice cap and Scottish ice is deflected by and retreats around the Outer Hebrides ice cap. An
590 ice sheet structure of local domes and far-travelled lobes (Stages 7-10) is similar to those proposed
591 for the Innuitan Ice Sheet (England *et al.*, 2006) and the deglacial stages of the Scandinavian Ice
592 Sheet over Denmark (Kjær *et al.*, 2003), and raises the question of whether some of the peripheral
593 ice domes were cold-based creating a networked basal thermal regime (e.g. Kleman and Glasser,
594 2007, Kleman and Hättestrand, 1999). Field evidence and modelling results show that the Welsh ice
595 cap was cold-based for much of the last glaciation, including low elevation sites, and particularly
596 when coupled to the Irish Sea ice lobe (Patton *et al.* 2013; Jansson and Glasser, 2004, 2008; Sahlin
597 *et al.* 2009). Mitchell (2008, 2007) describes evidence for cold-based ice on the Cheviots and the
598 northern Pennines, and the landscape of the Cairngorms has for a long time been ascribed to the
599 distribution of cold ice at the ice sheet bed (Sugden, 1968; Hall and Glasser, 2003). This conception
600 of retreat also explains the limited extension of Lake District and Cheviot sourced erratics and the
601 lack of foreign lithologies within these regions (Clark *et al.* 2004; Figs. 4b, 5). The presence of
602 cold-based ice close to the periphery of the ice sheet has implications for the position of the
603 southernmost limit in England. For example, cold-based ice could explain the apparent absence of
604 glacial deposits and landforms on the Cleveland Hills and Peak District and therefore support a
605 more southerly ice limit incorporating these areas. Terrestrial cosmogenic isotope dating from the
606 Island of Lundy has indicated that this location may have hosted a cold-based non-erosive ice cap
607 during the last glaciation (Rolfe *et al.* 2012).

608
609 Numerical and isostatic models of the last BIS have produced disparate values for the altitude of the
610 ice surface, largely reflecting uncertainties in the boundary conditions used, such as the nature of
611 the ice-sheet bed and the spatial extent. Values range from between 1800-1000 m and 1200-500 m
612 in central Scotland and North Wales respectively (Boulton *et al.* 1977, 1985, 1991), with more
613 recent models generating maximum elevations closer to the higher end of these ranges; 2250-1500
614 m (Boulton and Hagdorn, 2006) and 1200 m in Wales (Patton *et al.* 2013). Isostatic models

615 generate maximum values between 2500-1000 m (Lambeck, 1991, 1995; Johnston and Lambeck,
616 2000; Shennan *et al.*, 2002). Our results for an initial ‘thick’ ice sheet satisfies the demand of the
617 isostatic record and provides additional evidence to reject the interpretation of the mapped trimlines
618 as representing the highest elevation reached by the BIS during the last glacial (Kuchar *et al.* 2012).
619 That the oldest flowsets demand a persistent major N-S ice divide, defining the highest point on the
620 ice-sheet surface to sit within 100 km of previously proposed nunatak locations implies that the ice
621 sheet must have risen above these peaks during these stages. Presuming that surface profiles derived
622 from modern ice masses are a good analogue for past ice sheets, we use the formulae of Ng *et al.*
623 (2010) to calculate the minimum possible divide height based on the distance from the ice-sheet
624 margin to the reconstructed divide position. This approach reconstructs the divide over northern
625 Scotland during Stages 5-6 reaching at least 1400 m elevation, ~400 m higher than the highest
626 suggested trimline in northern Scotland (McCarroll *et al.* 1995; Ballantyne and Hallam, 2001). Over
627 northern England we calculate the minimum divide height to be 1000 m, ~100 m higher than the
628 highest proposed palaeonunatak in the Lake District (Lamb and Ballantyne, 1998). The observed
629 trimlines instead reflect either an englacial thermal boundary defining the extent of cold-based ice
630 on upland summits as concluded by Ballantyne (2010) and Fabel *et al.* (2012) or may be inherited
631 from a previous glaciation or represent the ice-sheet surface achieved following thinning prior to
632 marginal retreat (Stages 7-10). If the latter, the presence of trimlines may indicate that the ice
633 sheet had a low surface profile relative to relief for a significant proportion of the glacial cycle.

634
635 Our conception of a bi-modal ice-sheet geometry related to ice-surface elevation implies that the ice
636 loading distribution varied during the glaciation. At an early stage the centre of mass moves south,
637 but then settles over southwest Scotland and the North Channel until separation of the British and
638 Irish Ice Sheets. In our reconstruction, assuming ice divides coincide with greatest ice thickness,
639 western Scotland (together with Ireland) was the site of both most sustained ice loading during the
640 last glaciation slightly west of the locations predicted by existing isostatic modelling: northern Irish
641 Sea (Lambeck, 1995) and Midland Valley of Scotland (Shennan *et al.*, 2006). Scotland sustains
642 ‘thicker’ ice for longest, and the south-eastern parts are only briefly coherently integrated with the
643 rest of the ice sheet (Fig. 8). The dominance of the western side of the ice sheet is reflected in the
644 combined observations from the retreat pattern, flow patterns and dates; confluence of British and
645 Irish ice in the North Channel persisted until after deglaciation of the Irish Sea and southern part of
646 the ice sheet. The overall SW-NE orientation of the ice sheet parallel with the continental shelf edge
647 indicates that proximity to the North Atlantic precipitation source was essential to the persistence of
648 the BIS, and that the ice sheet itself created a rain shadow effect in the southeast, enhancing the
649 dominant west-east precipitation gradient over the British Isles (Chandler and Gregory, 1976). It is
650 therefore likely that the advance and retreat of the last British-Irish Ice Sheet was highly sensitive to
651 changes in precipitation patterns and the movement of the Polar Front (Scourse *et al.* 2009;
652 Happinen *et al.* 2010), as also appears to have been the case during earlier glaciations (Lee *et al.*
653 2012; Thierens *et al.* 2012).

654
655 Changes in flow-pattern geometry may both reflect and/or be a driver of changes in ice-sheet mass
656 balance. Increased mass loss from the ice sheet may have been driven by external factors, such as
657 sea level rise, changing precipitation patterns and/or temperatures, or internal ice dynamics. We
658 propose that ice streaming and calving appear crucial to the flow structure of the BIS and drive

659 transitions in the ice-sheet flow-pattern geometry (Fig. 9). Increasing IRD flux delivery west to the
660 Barra Fan at ~29-28 ka (Scourse *et al.* 2009) is consistent with ice reaching the shelf edge and the
661 development of the North Channel Ice Stream (Stage 4; 28-27 ka). Coupling and uncoupling with
662 Scandinavian-sourced ice in the North Sea led to pivoting of the primary BIS ice divide and abrupt
663 changes in orientation of ice flow over north Scotland and the North Sea (Fig 8; Stage 5). We
664 propose that the second major change in geometry, from a thick (relative to topography) integrated
665 ice sheet reaching the shelf edge with a simple ice-divide structure (Stage 5, ~27-26 ka) to a thin ice
666 sheet (relative to topography) comprising multiple ice centres (Stage 7, ~22 ka), was driven by ice-
667 surface lowering initiated by increased ice stream discharge (Pritchard *et al.* 2009). Break up of ice
668 in the North Sea by progressive opening up of an embayment (Bradwell *et al.* 2008a; Clark *et al.*
669 2012) facilitated ice streaming along the north-eastern sector of the ice sheet into the North Sea,
670 which was coeval with advancement of the Irish Sea Ice Stream and continued ice streaming in the
671 Minch and North Channel (Stage 6, ~24 ka). This led to increased calving and melt from the ice
672 sheet in multiple locations, lowering the surface profile to create a new ice sheet form. The flow-
673 pattern record thus illustrates one cycle of dynamic reorganisation (or binge-purge behaviour) as
674 predicted by numerical modelling (Hubbard *et al.* 2009). Greatest ice-mass loss from the British-
675 Irish Ice Sheet, quantified by using IRD volume as a proxy for iceberg discharge, occurred between
676 27-25 ka and 17-16 ka BP, with peak IRD flux occurring at 24 ka BP (Haapanieni *et al.* 2009;
677 Hibbert *et al.* 2010), coeval with the switch from a thick to thin ice-sheet geometry. This supports
678 our conceptualisation (Fig. 9) of bi-modal states for an ice sheet with and without significant
679 marine-terminating margins.

680
681

682 5. Conclusions

683

684 We have organised the complex and fragmentary terrestrial subglacial bedform record in Britain
685 into 10 snapshots of ice-flow configuration via a process of glaciological inversion (Fig. 8). The
686 process of systematic mapping followed by careful analysis of the pattern and distribution of
687 landforms facilitated untangling of individual flow events (Fig. 3, Table S1) and their relative order
688 (Table 2) and also generated new templates for flowset identification (Table 1). We are able to
689 explain 95% of the identified flowsets in a 10-stage model of ice-sheet flow-configuration
690 evolution. This would suggest that the observed subglacial bedform record (Hughes *et al.* 2010) is
691 almost entirely a product of the last glacial cycle. However we acknowledge that our chronology is
692 tentative and some older flowsets could be inherited from a previous glaciation.

693

694 Only a few flowsets are identifiable in the preserved record that constrain the build-up of the ice
695 sheet (Fig 8; Stages 1-3) but the oldest flowsets are large and topographically unconstrained and
696 record an ice mass of reasonable size and thickness centred over Highland Scotland. As ice
697 expands, more southerly ice masses, with the exception of the Welsh ice cap, are incorporated into
698 the main ice-sheet structure. During maximum glacial extent the centre of the ice sheet shifts south
699 and the ice sheet operates as an integrated ice mass with a primary N-S trending divide. Ice
700 streaming results in substantial shifts in the flow-pattern structure and the ice sheet assumes a shelf-
701 parallel orientation (Stages 4-6), which is maintained throughout retreat (Stages 7-10). Initial
702 thinning, interpreted as driven by ice stream activity, creates an ice sheet composed of multiple

703 domes and lobes with a complex basal-thermal structure, before final retreat to multiple locations
704 on the western side of the country. The main findings we draw from the reconstruction are:

- 705
706 1. Most flow patterns are indicative of ‘thin ice’ relative to basal topography and yield a multi-
707 domed ice sheet. The complexity of the flowsets in the central sector of the ice sheet reflects the
708 changing relative dominance and interaction of different ice domes, and confirms the British
709 subglacial landform record as a palimpsest archive of multiple ice-sheet geometries.
- 710 2. Some ice divides were persistent features but the majority were either transitory or experienced
711 substantial migrations in position (6-100 km).
- 712 3. The largest, most spatially extensive flowsets are satisfied by a large simple divide structure
713 which suggests that at its peak the last BIS must have been thick, the surface certainly clearing
714 the highest mountains. This finding strengthens the interpretation that high altitude erosion limits
715 in Scotland represent englacial thermal transitions, rather than the maximum surface height of
716 the last glacial ice sheet. Many of the formerly proposed nunatak sites lie close to or directly
717 below the reconstructed principle ice divide during the early stages of our model.
- 718 4. By teasing out discrete flowsets and their relative timing, we find that the last BIS had two main
719 modes of flow-pattern geometry (Fig. 9). A thick (relative to topography) integrated ice sheet
720 reaching the shelf edge with a simple ice-divide structure and a thin ice sheet (relative to
721 topography) comprising multiple ice centres and with a more complex flow structure. Such
722 changes in the distribution of ice mass during the last glacial have implications for
723 reconstructions of the isostatic loading history in Western Europe.
- 724 5. For large ice sheets such as the Laurentide and Fennoscandian, cross-cutting flow patterns
725 mostly appear to record migrations of ice divides, switching of ice streams (e.g. Boulton and
726 Clark, 1990; Clark *et al.* 2000), or patchy sticky-spot preservation (Trommelen *et al.* 2012). In
727 contrast, the complexity of flow patterns identified for the BIS (Fig. 3) almost precluded a
728 reconstruction using these ideas as templates (Section 2.3.3), until it was appreciated that for a
729 smaller (and thinner) ice sheet, basal topography plays a much larger role in determining ice
730 flow and much of the cross-cutting is actually a record of ice-thickness changes. Recognition of
731 these associations stimulated new templates for flow-pattern reconstruction (Table 1; TT
732 thinning) and a bi-modal configuration model for the last BIS (Fig. 9).
- 733 6. We infer that ice streams and break up of ice in the North Sea were key drivers of changes in ice-
734 sheet geometry and thickness.

735
736 We consider our 10-stage model to be the simplest interpretation of the information contained
737 within the geomorphological record of former ice-sheet flow patterns, and that it will serve as a
738 framework for more detailed studies. Reducing the uncertainty in the timing of changes in ice-sheet
739 geometry is critical to understanding the factors controlling the observed dynamic changes in ice
740 flow. This requires a sustained attempt to improve the ice-sheet margin chronology both for ice-
741 sheet retreat and build-up and integration of the geomorphological record with stratigraphic
742 observations at the ice-sheet scale (e.g. Livingstone *et al.* 2012; Finlayson *et al.* 2014). Further
743 advances will also be achieved by increasing the spatial coverage of offshore geomorphological
744 mapping (e.g. Dunlop *et al.* 2010; Howe *et al.* 2012). We have proposed simple explanations for the
745 changes in configuration of the ice sheet through time. An alternative, and more robust approach to
746 examine dynamic causes behind the observed changes in ice-flow geometry, would be to use the

747 building blocks or ingredients of our reconstruction (flowsets, retreat pattern and relative
748 chronology) as a test or input to improve and constrain numerical ice-sheet models (e.g. Li *et al.*
749 2007; Napieralski *et al.* 2007ab; Hubbard *et al.* 2009; Patton *et al.* 2013; Stokes *et al.* 2012) and we
750 provide a larger version of Fig. 3 and full documentation describing each flowset as supplementary
751 material (Fig. S1, Table S1). Such approaches in combination with glacial isostatic adjustment
752 modelling (e.g. Bradley *et al.* 2011) would also test our hypotheses regarding the controls on
753 changes in ice-sheet thickness, proposed locations of ice streams and cold-based ice and to
754 investigate the timing and duration of the observed ice-sheet flow-pattern configurations.

755
756

757 **Acknowledgements**

758 Mapping, flowset identification and initial reconstruction work formed part of the PhD thesis of
759 ALCH, conducted at the University of Sheffield (2004-2008) funded by a British Geological
760 Survey-NERC PhD Studentship (NER/S/A/2004/12102). Some additional work and writing was
761 conducted while ALCH was funded by the Leverhulme Trust (GLIMPSE Project) at Swansea
762 University (October 2008-December 2011) and in her present position at the University of Bergen
763 (January 2012-). We thank Sarah Greenwood and Jonathan Lee for their insightful comments and
764 Bethan Davies and Michelle Trommelen for their thorough reviews which improved the quality of
765 the manuscript. CJJ publishes with permission of the Executive Director of the British Geological
766 Survey.

767
768

769 **Supplementary Material**

770 Large version of the flowset map (Fig. S1).
771 Table describing each flowset (Table S1).

772
773

774 **References**

- 775 Arnold, N., Sharp, M. 2002. Flow variability in the Scandinavian ice sheet: modelling the coupling between
776 ice sheet flow and hydrology. *Quat. Sci. Rev.* 21, 485-502.
- 777 Ballantyne, C.K. 2010. Extent and deglacial chronology of the last British-Irish Ice Sheet: implications of
778 exposure dating using cosmogenic isotopes. *J. Quat. Sci.* 25, 515-534.
- 779 Ballantyne, C.K., Hallam, G.E. 2001. Maximum altitude of Late Devensian glaciation on South Uist, Outer
780 Hebrides, Scotland. *Proc. Geol. Assoc.* 112, 155-167.
- 781 Benn, D.I., Evans, D.J.A. 2010. *Glaciers and Glaciation* (2nd ed.). Hodder Education, London.
- 782 Boston, C.M., Evans, D.J., Cofaigh, C.Ó. 2010. Styles of till deposition at the margin of the Last Glacial
783 Maximum North Sea lobe of the British-Irish Ice Sheet: an assessment based on geochemical properties
784 of glacial deposits in eastern England. *Quat. Sci. Rev.* 29, 3184-3211.
- 785 Boulton, G.S., Clark, C.D. 1990. A highly mobile Laurentide Ice Sheet revealed by satellite images of glacial
786 lineations. *Nature*, 346, 813-817.
- 787 Boulton, G.S., Hagdorn, M.K. 2006. Glaciology of the British Isles Ice Sheet during the last glacial cycle:
788 form, flow, streams and lobes. *Quat. Sci. Rev.* 25, 3359-3390.
- 789 Boulton, G.S., Jones, A.S., Clayton, K.M., Kenning, M.J. 1977. A British ice sheet model and patterns of
790 glacial erosion and deposition in Britain and Ireland, In: Shotton, F. (Ed.), *British Quaternary Studies:*
791 *Recent advances.* Clarendon Press, Oxford.

- 792 Boulton, G.S., Peacock, J.D., Sutherland, D.G. 1991. Quaternary. In Craig, G.Y. (ed.) *The Geology of*
793 *Scotland*. Geol. Soc. Spec. Pub., London, 503-544.
- 794 Bradley, S.L., Milne, G.A., Shennan, I., Edwards, R. 2011. An improved glacial isostatic adjustment model
795 for the British Isles. *J. Quat. Sci.*, 26, 541–552.
- 796 Bradwell, T., Stoker, M., Larter, R. 2007. Geomorphological signature and flow dynamics of the Minch
797 palaeo-ice stream, northwest Scotland. *J. Quat. Sci.* 22, 609-617.
- 798 Bradwell, T., Stoker, M., Golledge, N., Wilson, C., Merritt, J., Long, D., Everest, J., Hestvik, O., Stevenson,
799 A., Hubbard, A., Finlayson, A., Mathers, H. 2008a. The northern sector of the last British Ice Sheet:
800 maximum extent and demise. *Earth Sci. Rev.* 88, 207-226.
- 801 Bradwell, T., Stoker, M.S., Krabbendam, K. 2008b. Megagrooves and streamlined bedrock in NW Scotland:
802 the role of ice streams in landscape evolution. *Geomorph.* 97, 135-156.
- 803 Chandler, T.J., Gregory, S. 1976. *The climate of the British Isles*. Longman, London.
- 804 Charlesworth, J.K. 1957. *The Quaternary Era*. Arnold, London.
- 805 Chiverrell, R.C., Thomas, G.S.P. 2010. Extent and timing of the Last Glacial Maximum (LGM) in Britain
806 and Ireland: A review. *J. Quat. Sci.* 25, 535-549.
- 807 Chiverrell, R.C., Thrasher, I.M., Thomas, G.S.P., Lang, A., Scourse, J.D., van Landeghem, K.J.J.,
808 McCarroll, D., Clark, C.D., Ó Cofaigh, C., Evans, D.J.A., Ballantyne, C.K. 2013. Bayesian modelling the
809 retreat of the Irish Sea Ice Stream. *J. Quat. Sci.* 28, 200-209.
- 810 Clapperton, C.M. 1970. The evidence for a Cheviot ice cap. *Trans. Inst. Br. Geogr.* 29, 31-45.
- 811 Clark, C.D. 1997. Reconstructing the evolutionary dynamics of former ice sheets using multi-temporal
812 evidence, remote sensing and GIS. *Quat. Sci. Rev.* 16, 1067-1092.
- 813 Clark, C.D. 1999. Glaciodynamic context of subglacial bedform generation and preservation. *Ann. Glaciol.*
814 28, 23-32.
- 815 Clark, C.D., Meehan, R.T. 2001. Subglacial bedform geomorphology of the Irish Ice Sheet reveals major
816 configuration changes during growth and decay. *J. Quat. Sci.* 16, 483-496.
- 817 Clark, C.D., Knight, J.K., Gray, J.T. 2000. Geomorphological reconstruction of the Labrador Sector of the
818 Laurentide Ice Sheet. *Quat. Sci. Rev.* 19, 1343-1366.
- 819 Clark, C.D., Evans, D.J., Khatwa, A., Bradwell, T., Jordan, C.J., Marsh, S.H., Mitchell, W.A., Bateman,
820 M.D. 2004. Map and GIS database of glacial landforms and features related to the last British Ice Sheet.
821 *Boreas* 33, 359-375.
- 822 Clark, C.D., Hughes, A.L.C., Greenwood, S.L., Jordan, C.J., Sejrup, H-P. 2012. Pattern and timing of retreat
823 of the last British-Irish Ice Sheet. *Quaternary Science Reviews*, 44, 112-146.
- 824 Davies, B. J., Roberts, D. H., Bridgland, D. R., Ó Cofaigh, C. 2012. Dynamic Devensian ice flow in NE
825 England: a sedimentological reconstruction. *Boreas*, 41, 337–366.
- 826 De Angelis, H., Kleman, J. 2005. Palaeo-ice streams in the northern Keewatin sector of the Laurentide ice
827 sheet. *Ann. Glaciol.* 42, 135-144.
- 828 De Angelis, H., Kleman, J. 2007. Palaeo-ice streams in the Foxe/Baffin sector of the Laurentide Ice Sheet.
829 *Quat. Sci. Rev.* 26, 1313-1331.
- 830 Dunlop, P., Clark, C.D., Hindmarsh, R.C.A. 2008. Bed Ribbing Instability Explanation: Testing a numerical
831 model of ribbed moraine formation arising from coupled flow of ice and subglacial sediment. *J. Geophys.*
832 *Res. - Earth Surface*, 113 (F03005), 1-15.
- 833 Dunlop, P., Shannon, R., McCabe, M., Quinn, R. and Doyle, E. 2010. Marine geophysical evidence for ice
834 sheet extension and recession on the Malin Shelf: New evidence for the western limits of the British Irish
835 Ice Sheet. *Marine Geol.* 276, 86-99.
- 836 England, J.H., Atkinson, N., Bednarski, J., Duyke, A.S., Hodgson, D.A., Ó Cofaigh, C. 2006. The Inuitian
837 Ice Sheet: configuration, dynamics and chronology. *Quat. Sci. Rev.* 25, 7-8.
- 838 Evans, D.J.A., Clark, C.D., Mitchell, W.A. 2005. The last British Ice Sheet: A review of the evidence
839 utilised in the compilation of the Glacial Map of Britain. *Earth Sci. Rev.* 70, 253-312.

840 Evans, D.J.A., Ó Cofaigh, C. 2003. Depositional evidence for marginal oscillations of the Irish Sea ice
841 stream in southeast Ireland during the last glaciation. *Boreas* 32, 76-101.

842 Evans, D.J.A, Livingstone, S.J., Vieli, A., Ó Cofaigh, C. 2009. The palaeoglaciology of the central sector of
843 the British and Irish Ice Sheet: reconciling glacial geomorphology and preliminary ice sheet modelling.
844 *Quat. Sci. Rev.* 28, 739-757.

845 Everest, J., Bradwell, T., Golledge, N. 2005. Subglacial Landforms of the Tweed Palaeo-Ice Stream. *Scott.*
846 *Geogr. J.* 121, 163-174.

847 Fabel, D., Ballantyne, C., Xu, S. 2012. Trimlines, blockfields, mountain-top erratics and the vertical
848 dimensions of the last British-Irish Ice Sheet in NW Scotland. *Quat. Sci. Rev.* 55, 91-102.

849 Finlayson, A., Merritt, J., Browne, M., Merritt, J.E., McMillan, A., Whitbread, K. 2010. Ice sheet advance,
850 dynamics, and decay configurations: evidence from west central Scotland. *Quat. Sci. Rev.* 29, 969-988.

851 Fitzpatrick, E.A. 1965. An interglacial soil at Teindland, Morayshire. *Nat.* 207, 621-622.

852 Geikie, J. 1894. *The Great Ice Age and its relation to the antiquity of man.* Edward Stanford, London.

853 Glasser, N.F., Hughes, P.D., Fenton, C., Schnabel, C. Rother, H. 2012. 10Be and 26Al exposure-age dating
854 of bedrock surfaces on the Aran Ridge, Wales: Evidence for a thick Welsh Ice Cap at the LGM. *J. Quat.*
855 *Sci.* 27, 97-104.

856 Golledge, N.R., Stoker, M. 2006. A palaeo-ice stream of the British Ice Sheet in eastern Scotland. *Boreas* 35,
857 231-243.

858 Graham, A.G.C., Lonergan, L., Stoker, M.S. 2007. Evidence for Late Pleistocene ice stream activity in the
859 Witch Ground Basin, central North Sea, from seismic reflection data. *Quat. Sci. Rev.* 26, 627-643.

860 Graham AGC, Lonergan L, Stoker MS. 2010. Depositional environments and chronology of Late
861 Weichselian glaciation and deglaciation in the central North Sea, *Boreas*, 39, pp. 471-491.

862 Greenwood, S.L., Clark, C.D. 2009a. Reconstructing the last Irish Ice Sheet 1: changing flow geometries and
863 ice flow dynamics deciphered from the glacial landform record. *Quat. Sci. Rev.* 28, 3085-3100.

864 Greenwood, S.L., Clark, C.D. 2009b. Reconstructing the last Irish Ice Sheet 2: a geomorphologically-driven
865 model of ice sheet growth, retreat and dynamics. *Quat. Sci. Rev.* 28, 3101-3123.

866 Hall, A.M., Glasser, N.F. 2003. Reconstructing the basal thermal regime of an ice stream in a landscape of
867 selective linear erosion: Glen Avon, Cairngorm Mountains, Scotland. *Boreas* 32, 191-207.

868 Haapaniemi, A.I., Scourse, J.D., Peck, V.L., Kennedy, H., Kennedy, P., Hemming, S.R., Furze, M.F. A.,
869 Pieńkowski, A.J., Austin, W.E. N., Walden, J., Wadsworth, E. Hall, I.R. 2010. Source, timing, frequency
870 and flux of ice-rafted detritus to the Northeast Atlantic margin, 30-12 ka: testing the Heinrich precursor
871 hypothesis. *Boreas*, 39, 576-591.

872 Hedges, R.E.M., Housley, R.A., Ramsey, C.B., Van Klinken, G.J. 1994. Radiocarbon-Dates from the Oxford
873 AMS System - Archaeometry Datelist- 18. *Archaeom.* 36, 337-374.

874 Hibbert, F.D., Austin, W.E.N., Leng, M.J., Gatliff, R.W. 2010. British Ice Sheet dynamics inferred from
875 North Atlantic ice-rafted debris records spanning the last 175 000 years. *J. Quat. Sci.*, 25, 461-482.

876 Hiemstra, J.F., Evans, D.J.A., Scourse, J.D., McCarroll, D., Furze, M.F.A., Rhodes, E. 2006. New evidence
877 for a grounded Irish Sea glaciation of the Isles of Scilly, UK. *Quat. Sci. Rev.* 25, 299-309.

878 Howe, J., Dove, D., Bradwell, T., Gafeira, J. 2012. Submarine geomorphology and glacial history of the Sea
879 of the Hebrides, Scotland. *Mar. Geol.* 315-318: 64-76.

880 Hubbard, A., Bradwell, T., Golledge, N., Hall, A., Patton, H., Sugden, D., Cooper, R., Stoker, M. 2009.
881 Dynamic cycles, ice streams and their impact on the extent, chronology and deglaciation of the British-
882 Irish ice sheet. *Quat. Sci. Rev.* 28, 758-776.

883 Hughes, A.L.C. 2009. *The last British Ice Sheet: a reconstruction based on glacial landforms.* Unpublished
884 PhD thesis, University of Sheffield.

885 Hughes, A.L.C., Clark, C.D., Jordan, C.J. 2010. Subglacial bedforms of the last British Ice Sheet. *J. Maps*,
886 v2010, 543-563.

- 887 Hughes, A.L.C., Greenwood, S.L., Clark, C.D. 2011. Dating constraints on the last British-Irish Ice Sheet: a
888 map and database, *J. Maps*, v2011, 156-183.
- 889 Jamieson, S.S.R., Vieli, A., Livingstone, S.J., Ó Cofaigh, C., Stokes, C.R., Hillenbrand, C-D., Dowdeswell,
890 J.A. 2012. Ice-stream stability on a reverse bed slope. *Nature Geoscience* 5, 799–802.
- 891 Jansson, K.N., Glasser, N.F. 2004. Palaeoglaciology of the Welsh sector of the British-Irish Ice Sheet. *J.*
892 *Geol. Soc. Lond.* 161, 1-13.
- 893 Jansson, K.N., Glasser, N.F. 2008. Modification of peripheral mountain ranges by former ice sheets: The
894 Brecon Beacons, southern UK. *Geomorphol.* 97, 178-189.
- 895 Jardine, W.G., Dickson, J.H., Haughton, P.D.W., Harkness, D.D., Bowen, D.Q., Sykes, G.A. 1988. A Late
896 middle Devensian interstadial site at Sourlie, near Irvine, Strathclyde. *Scott. J. Geol.* 24, 288-295.
- 897 Johnston, P.J., Lambeck, K. 2000. Automatic inference of ice models from postglacial sea level
898 observations: Theory and application to the British Isles. *J. Geophys. Res.* 105, 13179-13194.
- 899 Kjær, K.H., Houmark-Nielsen, M., Richardt, N. 2003. Ice-flow patterns and dispersal of erratics at the
900 southwestern margin of the last Scandinavian Ice Sheet: signature of palaeo-ice streams. *Boreas* 32, 130-
901 148.
- 902 Kleman, J., Borgström, I. 1996. Reconstruction of palaeo-ice sheets: the use of geomorphological data. *Earth*
903 *Surf. Process. Landf.* 21, 893-909.
- 904 Kleman, J., Hättestrand, C. 1999. Frozen-bed Fennoscandian and Laurentide ice sheets during the Last
905 Glacial Maximum. *Nat.* 402, 63-66.
- 906 Kleman, J., Glasser, N.F. 2007: Subglacial Thermal Organization (STO) of Ice Sheets. *Quat. Sci. Rev.* 26,
907 585-597.
- 908 Kleman, J., Hättestrand, C., Borgström, I., Stroeven, A. 1997. Fennoscandian palaeoglaciology reconstructed
909 using a glacial geological inversion model. *J. Glaciol.* 43, 283-299.
- 910 Kleman, J., Hättestrand, C., Stroeven, A.P., Jansson, K.N., De Angelis, H., Borgström, I. 2006.
911 Reconstruction of paleo-ice sheets-inversion of their glacial geomorphological record, In: Knight, P.G.
912 (Ed.), *Glacier science and environmental change*. Blackwell Science Ltd, Oxford, pp. 192-198.
- 913 Kuchar, J., Milne, G., Hubbard, A., Patton, H., Bradley, S., Shennan, I., Edwards, R. 2012. Evaluation of a
914 numerical model of the British–Irish ice sheet using relative sea-level data: implications for the
915 interpretation of trimline observations. *J. Quat. Sci.*, 27: 597–605.
- 916 Lamb, A.L., Ballantyne, C.K. 1998. Paleonunataks and the altitude of the last ice sheet in the south-west
917 Lake District, England. *Proc. Geol. Soc.* 109, 305-316.
- 918 Lambeck, K. 1991. A model for Devensian and Flandrian glacial rebound and sea-level change in Scotland,
919 In: Sabadini, R., Lambeck, K., Boschi, E. (Eds.), *Glacial isostasy, sea level and mantle rheology*. Kluwer
920 Academic Publishers, Dordrecht.
- 921 Lambeck, K. 1995. Late Devensian and Holocene shorelines of the British Isles and North Sea from models
922 of glacio-hydro-isostatic rebound. *J. Geol. Soc. Lond.* 152, 437-448.
- 923 Lawson, T.J. 1984. Reindeer in the Scottish Quaternary. *Quat. Newsl.* 42, 1-7.
- 924 Lee, J.R., Busschers, F.S., Sejrup, H.P. 2012. Pre-Weichselian Quaternary glaciations of the British Isles,
925 The Netherlands, Norway and adjacent marine areas south of 68°N: implications for long-term ice sheet
926 development in northern Europe. *Quat. Sci. Rev.*, 44, 213-228.
- 927 Letzer, J.M. 1987. Drumlins of the southern Vale of Eden, In: Ehlers, J., Gibbard, P.L., Rose, J. (Eds.),
928 *Glacial deposits in Great Britain and Ireland*. Balkema, Rotterdam, pp. 323-334.
- 929 Li, Y., Napieralski, J., Harbor, J., Hubbard, A. 2007. Identifying patterns of correspondence between
930 modeled flow directions and field evidence: An automated flow direction analysis. *Comput. Geosci.* 33,
931 141-150.
- 932 Livingstone, S.J., Ó Cofaigh, C., Evans, D.J.A. 2008. The glacial geomorphology of the central sector of the
933 British-Irish Ice Sheet. *J. Maps*, v2008, 358-377.

- 934 Livingstone, S.J., Ó Cofaigh, C., Evans, D.J.A. 2010a. A major ice drainage pathway of the last British-Irish
935 Ice Sheet: the Tyne Gap, northern England. *J. Quat. Sci.* 25, 354-370.
- 936 Livingstone, S.J., Ó Cofaigh, C., Evans, D.J.A., Palmer, A. 2010b. Sedimentary evidence for a major glacial
937 oscillation and proglacial lake formation in the Solway Lowlands (Cumbria, UK) during Late Devensian
938 deglaciation. *Boreas*, 39, 505-527.
- 939 Livingstone, S.J., Evans, D.J.A., Ó Cofaigh, C. 2010c. Re-advance of Scottish Ice into the Solway Lowlands
940 (Cumbria, UK) during the Main Late Devensian deglaciation. *Quat. Sci. Rev.* 29, 2544-2570.
- 941 Livingstone, S.J., Evans, D.J.A., Ó Cofaigh, C., Davies, B.J., Merritt, J.W., Huddart, D., Mitchell, W.A.,
942 Roberts, D.H., Yorke, L. 2012. Glaciodynamics of the central sector of the last British-Irish Ice Sheet in
943 Northern England. *Earth Sci. Rev.* 111, 25-55.
- 944 McCarroll, D., Ballantyne, C.K., Nesje, A., Dahl, S.O. 1995. Nunataks of the last ice sheet in northwest
945 Scotland. *Boreas* 24, 305-323.
- 946 McCarroll, D., Stone, J.O., Ballantyne, C.K., Scourse, J.D., Fifield, L.K., Evans, D.J.A., Hiemstra, J.F. 2010.
947 Exposure-age constraints on the extent, timing and rate of retreat of the last Irish Sea ice stream. *Quat.*
948 *Sci. Rev.* 29, 1844-1852.
- 949 Merritt, J.W., Auton, C.A., Firth, C.R. 1995. Ice-proximal glaciomarine sedimentation and sea-level change
950 in the Inverness area, Scotland: a review of the deglaciation of a major ice stream of the British late
951 Devensian ice sheet. *Quat. Sci. Rev.* 14, 289-329.
- 952 Mitchell, W.A. 1994. Drumlins in ice-sheet reconstructions, with reference to the western Pennines, northern
953 England. *Sediment. Geol.* 91, 313-331.
- 954 Mitchell, W.A. 2007. Reconstructions of the Late Devensian (Dimlington Stadial) British-Irish Ice Sheet: the
955 role of the upper Tees drumlin field, north Pennines, England. *Proc. Yorks. Geol. Soc.* 56, 221-234.
- 956 Mitchell, W.A. 2008. Quaternary Geology of part of the Kale Water catchment, Western Cheviot Hills,
957 southern Scotland. *Scottish J. Geol.* 44, 51-63.
- 958 Napieralski, J., Harbor, J., Li, Y. 2007a. Glacial geomorphology and geographic information systems. *Earth*
959 *Sci. Rev.* 85, 1-22.
- 960 Napieralski, J., Hubbard, A., Li, Y., Harbor, J., Stroeven, A.P., Kleman, J., Alm, G., Jansson, K.N. 2007b.
961 Towards a GIS assessment of numerical ice-sheet model performance using geomorphological data. *J.*
962 *Glaciol.* 53, 71-83.
- 963 Ng, F., Barr, I.D., Clark, C.D. 2010. Using the surface profiles of modern ice masses to inform palaeo-
964 glacier reconstruction. *Quat. Sci. Rev.* 29, 3240-3255.
- 965 Ó Cofaigh, C., Evans, D.J.A. 2007. Radiocarbon constraints on the age of the maximum advance of the
966 British-Irish Ice Sheet in the Celtic Sea. *Quat. Sci. Rev.* 26, 1197-1203.
- 967 Patton, H., Hubbard, A., Glasser, N.F., Bradwell, T., Golledge, N.R. 2013. The last Welsh Ice Cap: Part 2 –
968 Dynamics of a topographically controlled ice cap. *Boreas*. 42, 491–510.
- 969 Peck, V.L., Hall, I.R., Zahn, R., Elderfield, H., Grousset, F., Hemming, S.R., Scourse, J.D. 2006. High
970 resolution evidence for linkages between NW European ice sheet instability and Atlantic Meridional
971 Overturning Circulation. *Earth Planet. Sci. Lett.* 243, 476-488.
- 972 Pinson, L.J.W., Vardy, M.E., Dix, J.K., Henstock, T.J., Bull, J.M., MacLachlan, S.E. 2013. Deglacial history
973 of glacial lake Windermere, UK; implications for the central British and Irish Ice Sheet. *J. Quat. Sci.*, 28,
974 83-94.
- 975 Pritchard, H.D., Arthern R.J., Vaughan, D.G., Edwards, L.A. 2009. Extensive dynamic thinning on the
976 margins of the Greenland and Antarctic ice sheets. *Nature*, 461, 971-975.
- 977 Rignot, E., Mouginot, J., Scheuchl, B. 2011. Ice Flow of the Antarctic Ice Sheet. *Science*, 333, 1427-1430.
- 978 Roberts, D.H., Dackombe, R.V., Thomas, G.S.P. 2007. Palaeo ice streaming in the central sector of the
979 British-Irish Ice Sheet during the Last Glacial Maximum: evidence from the northern Irish Sea Basin.
980 *Boreas*. 36, 115-129.

- 981 Roberts, D.H., Evans, D.J.A., Lodwick, J., Cox, N.J. 2013. The subglacial and ice-marginal signature of the
982 North Sea Lobe of the British–Irish Ice Sheet during the Last Glacial Maximum at Upgang, North
983 Yorkshire, UK. *Proc. Geol. Assoc.*, 124, 503-519.
- 984 Rolfe, C.J., Hughes, P.D., Fenton, C.R., Schnabel, C., Xu, S., Brown, A.G. 2012. Paired ¹⁰Be and ²⁶Al
985 exposure ages from Lundy: new evidence for the extent and timing of Devensian glaciation in the
986 southern British Isles. *Quat. Sci. Rev.* 43, pp. 61-73.
- 987 Rose, J., Letzer, J.M. 1977. Superimposed drumlins. *J. Glaciol.* 18, 471-480.
- 988 Sahlin, E.A.U., Glasser, N. F., Jansson, K. N., Hambrey, M. J. 2009: Connectivity analyses of valley patterns
989 indicate preservation of a preglacial fluvial valley system in the Dyfi basin, Wales. *Proc. Geol. Assoc.*
990 120, 245–255.
- 991 Salt, K.E., Evans, D.J.A. 2005. Superimposed subglacially streamlined landforms of southwest Scotland.
992 *Scott. Geogr. J.* 120, 133-147.
- 993 Scourse, J.D., Furze, F.A. 2001. A critical review of the glaciomarine model for Irish Sea deglaciation:
994 evidence from southern Britain, the Celtic shelf and adjacent continental slope. *J. Quat. Sci.* 16, 419-434.
- 995 Scourse, J.D., Haapaniemi, A.I., Colmenero-Hidalgo, E., Peck, V.L., Hall, I.R., Austin, W.E.N., Knutz, P.C.,
996 Zahn, R. 2009. Growth, dynamics and deglaciation of the last British-Irish Ice Sheet: the deep-sea ice-
997 rafted detritus record. *Quat. Sci. Rev.* 28, 3066-3084.
- 998 Sejrup, H.P., Haflidason, H., Aarseth, I., King, E., Forsberg, C.F., Long, D., Rokoengen, K. 1994. Late
999 Weichselian glaciation history of the northern North Sea. *Boreas* 23, 1-13.
- 1000 Shennan, I., Bradley, S., Milne, G., Brooks, A., Bassett, S., Hamilton, S. 2006. Relative sea-level changes,
1001 glacial isostatic modelling and ice-sheet reconstructions from the British Isles since the Last Glacial
1002 Maximum. *J. Quat. Sci.* 21, 585-599.
- 1003 Shennan, I., Peltier, W.R., Drummond, R., Horton, B. 2002. Global to local scale parameters determining
1004 relative sea level changes and the post glacial isostatic adjustment of Great Britain. *Quat. Sci. Rev.* 21,
1005 397-408.
- 1006 Sissons, J.B. 1967. *The Evolution of Scotland's Scenery*. Oliver and Boyd, Edinburgh.
- 1007 Smith, M.J., Knight, J. 2011. Palaeoglaciology of the last Irish ice sheet reconstructed from striae evidence.
1008 *Quat. Sci. Rev.*, 30, 147-160.
- 1009 Stoker, M.S., Bradwell, T. 2005. The Minch palaeo-ice stream, NW sector of the British-Irish Ice Sheet. *J.*
1010 *Geol. Soc. Lond.* 163, 425-428.
- 1011 Stoker, M S, Bradwell, T, Howe, J A, Wilkinson, I P, McIntyre, K. 2009. Lateglacial ice-cap dynamics in
1012 NW Scotland: evidence from the fjords of the Summer Isles region. *Quat. Sci. Rev.* 28, 3161-3184.
- 1013 Stokes, C.R., Clark, C.D. 1999. Geomorphological criteria for identifying Pleistocene ice streams. *Ann.*
1014 *Glaciol.* 28, 67-75.
- 1015 Stokes, C.R., Tarasov, L., Dyke, A.S. 2012. Dynamics of the North American Ice Sheet Complex during its
1016 inception and build-up to the Last Glacial Maximum. *Quat. Sci. Rev.* 50, 86-104.
- 1017 Sugden, D.E. 1968. The selectivity of glacial erosion in the Cairngorm Mountains, Scotland. *Trans. Inst. Br.*
1018 *Geogr.* 45, 79-92.
- 1019 Sutherland, D.G. 1984. The Quaternary deposits and landforms of Scotland and the neighbouring shelves: a
1020 review. *Quat. Sci. Rev.* 3, 157-254.
- 1021 Sutherland, D.G., Ballantyne, C.K., Walker, M.J.C. 1984. Late Quaternary glaciation and environmental
1022 change on St-Kilda, Scotland and their paleoclimatic significance. *Boreas* 13, 261-272.
- 1023 Sutherland, D.G., Walker, M.J.C. 1984. A late Devensian ice-free area and possible interglacial site on the
1024 Isle of Lewis, Scotland. *Nat.* 309, 701-703.
- 1025 Thierens, M., Pirlet, H., Colin, C., Latruwe, K., Vanhaecke, F., Lee, J.R., Stuut, J.-B., Titschack, J.,
1026 Huvenne, V.A.I., Dorschel, B., Wheeler, A.J., Henriot, J.-P. 2012. Ice-rafting from the British-Irish ice
1027 sheet since the earliest Pleistocene (2.6 million years ago): implications for long-term mid-latitude ice-
1028 sheet growth in the North Atlantic region. *Quat. Sci. Rev.* 44, 229-240.

- 1029 Toucanne, S., Zaragosi, S., Bourillet, J-F., Marieu, V., Cremer, M., Kageyama, M. Van Vliet-Lanoë, B.,
1030 Eynaud, F., Turon, J-L., Gibbard, P.L. 2010. The first estimation of Fleuve Manche palaeoriver discharge
1031 during the last deglaciation: Evidence for Fennoscandian ice sheet meltwater flow in the English Channel
1032 ca 20–18 ka ago, *Earth. Planet. Sci. Lett.*, .290, 459-473.
- 1033 Trommelen, M., Ross, M., Campbell, J.E. 2012. Glacial terrain zone analysis of a fragmented
1034 paleoglacialogic record, southeast Keewatin sector of the Laurentide Ice Sheet. *Quat. Sci. Rev.*, 40, 1-20.
- 1035 van Landeghem, K.J.J., Wheeler, A.J., Mitchell, N. 2009. Seafloor evidence for palaeo-ice streaming and
1036 calving of the grounded Irish Sea Ice Stream: implications for the interpretation of its final deglaciation
1037 phase. *Boreas*, 38, 119-131.
- 1038 Von Weymarn, J., Edwards, K. J. 1973. Interstadial site on the Island of Lewis. *Nature*. 246, 473–474.
- 1039 Wilson, L.J., Austin, W.E.N., Jansen, E. 2002. The last British Ice Sheet: growth, maximum extent and
1040 deglaciation. *Polar Res.* 21, 243-250.
- 1041 Wright, W.B. 1914. *The Quaternary Ice Age*. The Macmillan Co., New York.

1042 **Tables**

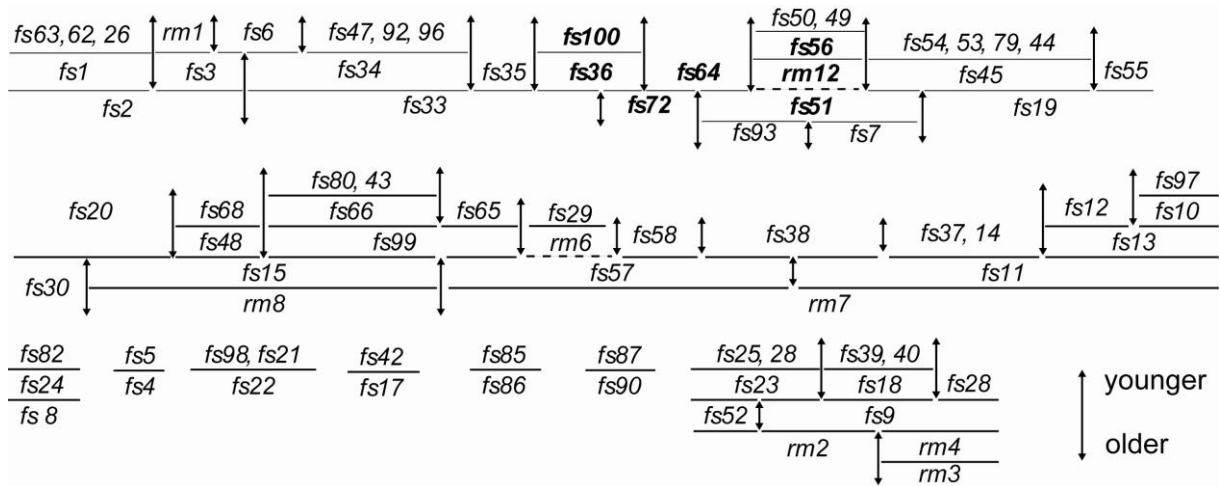
1043

1044 **Table 1** Flowset classification templates used in this reconstruction developed from Boulton and Clark (1990), Kleman
 1045 and Borgström (1996), Kleman *et al.* (1997, 2006), Clark (1999), Stokes and Clark (1999), Greenwood and
 1046 Clark (2009a). Key characteristics for each type listed as dashed bullet points, additional characteristics with a
 1047 ‘+’.
 1048

| Flowset classification | Bedform properties | Landform associations | Glaciodynamic context |
|---|--|---|--|
| Isochronous <i>'rubber-stamped' imprint</i> | <ul style="list-style-type: none"> - no cross cutting within flowset - high lineation parallel conformity - may ignore local topography - gradual trends in lineation morphometry and distribution | <ul style="list-style-type: none"> - no aligned eskers - no association with end moraines | <ul style="list-style-type: none"> - internal rather than marginal flow patterns - stable flow directions - range of ice thicknesses - warm based = <i>Ice sheet interior: sheet flow</i> |
| | <ul style="list-style-type: none"> + highly attenuated lineations + abrupt lateral margins + highly convergent flow patterns | <ul style="list-style-type: none"> + lateral shear moraines + trough mouth fans | <ul style="list-style-type: none"> + order of magnitude faster ice velocity = <i>Ice sheet interior: stream flow</i> |
| Time-transgressive (TT) <i>'smudged' imprint</i> | <ul style="list-style-type: none"> - lower parallel conformity of lineations - cross-cutting bedforms within flowset - abrupt spatial discontinuities in lineation morphometry and distribution | | <ul style="list-style-type: none"> - changing flow geometry due to divide migration - changing flow geometry due to outlet migration - warm based = <i>Flow-line migration</i> |
| | <ul style="list-style-type: none"> + elements of pattern correspond to local topography + cross-cutting is clustered around topographic obstacles | | <ul style="list-style-type: none"> - ice surface altitude decreases/increases relative to local topography - warm based = <i>Thinning/thickening ice</i> |
| | <ul style="list-style-type: none"> + pattern corresponds to local topography + lobate/splaying pattern | <ul style="list-style-type: none"> + aligned with eskers + associated with end moraines | <ul style="list-style-type: none"> - rapidly varying flow directions - thin ice - sheet or stream flow - warm based = <i>Behind retreating ice sheet margin 'wet-bed'</i> |
| | <ul style="list-style-type: none"> - absence of bedforms: landform record dominated by meltwater channels | <ul style="list-style-type: none"> - lateral meltwater channels: pattern constrained by local topography | <ul style="list-style-type: none"> - topographically constrained - sheet flow - frozen bed - thin ice = <i>Behind retreating ice margin 'dry-bed'</i> |

1049
 1050
 1051
 1052
 1053
 1054
 1055
 1056
 1057
 1058

Table 2 Flowset relative-age chronology. Horizontal lines separate flowsets that are known to be older or younger than each other, as determined from superimposition of the constituent subglacial bedforms, with the youngest flowsets shown at the top and oldest at the bottom. Many flowsets are laterally adjacent but do not overlap meaning that no relative-age relationship can be defined. Flowsets and/or flowset groups that have no definitive chronological relationship are separated by vertical arrows to demonstrate the uncertainty in their relative timing: e.g. *fs64* and *fs36* are both older than *fs72*, but *fs64* could be either older, younger or the same age as *fs36* and *fs100*. Dotted horizontal lines mean there is no direct relationship between the two flowsets: e.g. *fs56* overprints *rm12* and *fs51*, but *rm12* has no relationship with *fs51*. Flowset numbers are the same as in Fig. 3 and Table S1.



1059
 1060
 1061

1062
1063
1064

Table 3 Flowset and ancillary evidence groupings underpinning each stage of the reconstruction model (Fig. 8). Five small flowsets do not fit within the model and may be inherited from a previous glaciation (*fs96*, *fs97*, *fs92*, *fs35* and *fs93*). TT = Time Transgressive.

| | Flowset grouping | Security of interpretation |
|------------------------------------|---|---|
| Stage 1 | <i>fs2</i> , <i>fs33</i> <i>fs7</i> <i>rm13</i> | Large <i>flowsets</i> , little relationship with topography, stratigraphically oldest in Scotland. <i>Fs7</i> is stratigraphically old and so included here, if relative chronology ignored it could be included in Stage 5. <i>Rm13</i> is placed here as is aligned with flow direction of <i>fs2</i> . Could be earlier or later; no superimposition information. |
| Stage 2 | <i>fs2</i> , <i>fs33</i> <i>fs52</i> <i>rm2</i> , <i>rm3</i> <i>rm7</i> <i>rm6</i> | <i>Fs33</i> exhibits some smudging, interpreted as due to minor divide migration between Stages 1-2. Southern Upland and Highland ice connected, Highland ice is deflected around southern ice mass. <i>Fs52</i> is a large but exhibits signature of thinning/thickening. Placement reverses stratigraphic relationship with <i>fs19</i> , although this relation is equivocal. <i>Rm3</i> and <i>rm2</i> document NE-SW ice flow over Rhins of Galloway and Ayrshire. <i>Rm3</i> precedes <i>rm4</i> . <i>Rm2</i> probable southwest extension of <i>fs52</i> ; occurs just prior to <i>fs52</i> . <i>Rm7</i> must occur before other ice flow signatures in Solway lowlands, uncertain ice flow direction interpreted as broadly W-E. <i>Rm6</i> shows SE ice flow from a source over western Southern Uplands, could be earlier. |
| Stage 3 | <i>fs8</i> , <i>fs57</i> <i>rm9</i> | Isochronous flowsets, direction supported by streamlined bedrock, erratics and subglacial meltwater (<i>fs57</i>). <i>Fs8</i> identified as part of inferred North Channel Ice Stream. Lake District sourced ice expands to south; occurs prior to <i>fs31</i> . |
| Stage 4 | <i>fs19</i> <i>fs15</i> , <i>fs30</i> , <i>fs11</i> <i>fs22</i> <i>rm4</i> | <i>Fs19</i> identified as potential ice stream (Forth Ice Stream) based on parallel conformity and convergent pattern. Flow direction supported by erratics. Exhibits signature of thinning/thickening but must occur after <i>fs7</i> and before <i>fs52</i> , <i>fs55</i> , <i>fs45</i> . Major W-E ice flow over Northern England. All exhibit signs of thinning/thickening. Interpret this as due to proximity to ice margin. Also W-E ice flow over north-east Wales, no signature of thinning, independent of topography. <i>Rm4</i> must occur after <i>rm3</i> and before <i>fs9</i> . |
| Stage 5 | <i>fs1</i> , <i>fs34</i> , <i>fs59</i> <i>fs13</i> (<i>fs7</i>) <i>fs9</i> <i>fs17</i> , (<i>fs22</i>) <i>rm10</i> | Large and independent of topography indicating thick ice sheet and considerable offshore extent. <i>Fs59</i> interpreted as extension of <i>fs1</i> . Invoke connection with ice over North Sea due to deflection of ice flow over Scotland to NNE. Supported by streamlined bedrock and presence of shelly till on Caithness. Slight smudging in <i>fs1</i> and <i>fs34</i> indicates slight migration of divides. <i>Fs13</i> small flowset but with high parallel conformity, streamlined bedrock and subglacial meltwater traces support flow direction. <i>Fs7</i> could be placed here if ignore relative chronology. This would make Stage 1 unnecessary. <i>Fs9</i> cannot be placed with <i>fs8</i> or <i>fs19</i> . <i>Fs9</i> large flowset difficult to fit into any configuration, possible that more than one ice flow event with very similar flow directions represented, indicated by the variety of bedform size populations. Streamlined bedrock and erratics support flow direction. High parallel conformity and independent of topography. Ice flow to SE over Yorkshire Dales. |
| Stage 6 | <i>fs4</i> <i>fs31</i> <i>fs51</i> <i>fs90</i> , <i>fs78</i> <i>fs18</i> , <i>fs84</i> <i>fs86</i> | <i>Fs4</i> supported by streamlined bedrock directions, interpreted as tributaries of Minch Ice Stream (<i>fs4</i>) which appears as a relatively stable feature that can be incorporated into several configurations. Large flowset supported by streamlined bedrock, some expression of thinning but independent of topography during this stage. Large flowset, independent of topography, some minor smudging interpreted as due to divide migration. Potential ice stream (Strathmore I), but lacks abrupt margins and convergent flow patterns. Based on only a few drumlins, but consistent flow directions for this stage. Ice flow converges into northern Irish Sea; some smudging suggests minor fluctuations of flow patterns. Streamlined bedrock supports flow directions. Could also be grouped with <i>fs17</i> (Stage 5) and <i>fs99</i> (Stage 7). <i>Fs84</i> southward extension of <i>fs18</i> Small isochronous flowset, must occur before <i>fs85</i> . |
| Stage 6-7 | <i>fs16</i> , <i>fs77</i> | Retreat flowsets document separation of Welsh and Irish Sea ice by retreat out of Cheshire Plain as Irish Sea Ice stream steps back. Aligned with moraines and lobate patterns thus close to retreating margin. <i>Fs16</i> occurs before <i>fs69</i> and after <i>fs31</i> . |
| Stage 7 TT stage | <i>fs3</i> <i>fs72</i> <i>fs42</i> <i>fs21</i> , <i>fs76</i> , <i>fs60</i> <i>fs10</i> , <i>fs99</i> , <i>fs69</i> , <i>fs18</i> <i>fs20</i> <i>fs62</i> , <i>fs75</i> , <i>fs87</i> , <i>fs91</i> <i>rm11</i> , <i>rm1</i> | Ice flow converges to the coast and exhibits some evidence of thinning/thickening, streamlined bedrock and erratic paths are aligned and suggest extension of flow pattern to south. Must occur after <i>fs2</i> . Minor orientation changes interpreted as due to changes in the ice divide position. Bedrock supports ice flow direction. Lobate pattern suggests close to retreating margin. Topographically constrained ice flow, streamlined bedrock supports ice flow direction. Isochronous <i>flowsets</i> interpreted as ice streams/ice stream tributaries. Topographically constrained but high parallel conformity. Subglacial meltwater aligned. <i>fs10</i> necessitates branching of Southern Uplands ice divide. Necessitates divide over Pennines. Concordant with moraines and eskers, interpret as close to retreating ice margin. Small <i>flowsets</i> . Tentatively placed in this stage. W-E ice flow in Central Scotland (<i>rm11</i>). <i>Rm1</i> documents topographically constrained ice flow broadly W-E, aligned with <i>fs3</i> and confined to valley settings. |
| Stage 8 TT stage | <i>fs5</i> , <i>fs94</i> , <i>fs39</i> , <i>fs40</i> , <i>fs58</i> , <i>fs48</i> <i>fs36</i> <i>fs66</i> <i>fs70</i> <i>fs80</i> <i>fs83</i> , <i>fs74</i> , <i>fs85</i> , <i>fs98</i> , <i>fs32</i> , <i>fs41</i> , <i>fs43</i> , <i>fs68</i> , <i>fs71</i> , <i>fs89</i> , <i>fs73</i> <i>rm12</i> | Topographically constrained spatially restricted <i>flowsets</i> with smudging due to thinning. High parallel conformity, could fit into stage 4 or 6, but must be younger than <i>fs33</i> and <i>fs72</i> . Older than <i>fs100</i> . Aligned esker and smudging so interpreted as deglacial flowset. Younger than <i>fs99</i> . High parallel conformity, but topographically constrained. Must occur after <i>fs69</i> . High parallel conformity, younger than <i>fs66</i> , possibly represents readvance. Topographically constrained and/or deglacial <i>flowsets</i> that follow the above <i>flowsets</i> in northern England and document topographically constrained retreat back to local upland ice centres. <i>Fs32</i> , <i>fs41</i> , <i>fs43</i> , <i>fs68</i> , <i>fs71</i> , <i>fs89</i> , <i>fs80</i> and <i>fs73</i> occur at end of this time-transgressive stage but before Stage 9. Must occur before <i>fs56</i> . |
| Stage 9 | <i>fs6</i> , <i>fs100</i> <i>fs12</i> , <i>fs56</i> , <i>fs61</i> , <i>fs45</i> , <i>fs64</i> <i>fs14</i> <i>fs24</i> <i>fs25</i> , <i>fs29</i> <i>fs65</i> <i>fs63</i> , <i>fs95</i> , <i>fs88</i> <i>fs37</i> , <i>fs38</i> | Convergent ice flow into Moray Firth, interpreted as an ice stream. High elongation ratios and parallel conformity. Topographically constrained ice flow and thinning. <i>Fs56</i> is interpreted as possible ice stream (Strathmore II) and could occur in Stage 8. High parallel conformity, isochronous flowset, surge type fan (Kleman and Borgström, 1996). Occurs after <i>fs11</i> and close to ice sheet margin. Erratics and meltwater traces support flow directions. Deglacial <i>flowsets</i> with evidence of thinning. Retreat from Solway Firth. Small <i>flowsets</i> placed here as fit with overall ice flow patterns. Retreat to south and around Cheviots. Occur between Stage 9 and Stage 10. |
| Stage 10 TT stage | <i>fs23</i> <i>fs27</i> <i>fs82</i> , <i>fs81</i> , <i>fs67</i> , <i>fs26</i> , <i>fs46</i> , <i>fs47</i> , <i>fs49</i> , <i>fs50</i> , <i>fs53</i> , <i>fs54</i> , <i>fs55</i> , <i>fs79</i> , <i>fs28</i> <i>fs44</i> | Topographically constrained, flows offshore. Must occur prior to <i>fs28</i> and cannot occur contemporaneously with <i>fs25</i> . Deglacial flowset with lobate pattern, based on streamlined bedrock. Small, topographically constrained or deglacial <i>flowsets</i> . <i>Fs67</i> and <i>fs81</i> cannot have occurred at the same time although both part of the deglacial signature. Very high parallel conformity, topographically constrained, clearly superimposes <i>fs23</i> and <i>fs9</i> . Possible readvance of Highland ice during uncoupling. Lobate pattern within Loch Lomond limit and so probably relates to this stage. |

1065
1066
1067
1068
1069
1070
1071
1072
1073
1074
1075
1076
1077
1078
1079
1080
1081
1082
1083
1084
1085
1086
1087
1088
1089
1090
1091
1092
1093
1094
1095
1096
1097
1098
1099
1100
1101
1102
1103
1104
1105
1106
1107
1108
1109
1110
1111
1112
1113
1114
1115
1116

Figure captions

Figure 1 (a) Generalised flow patterns (arrows) of the last British-Irish Ice Sheet at its maximum extent (dashed line) as synthesised by Wright (1914) (redrawn from Boulton *et al.* 1977). (b) Map of British Isles. Key locations mentioned in the text are marked: A=Ayrshire, C=Caithness, Cg=Cairngorm, Ch=Cheviots, CH= Cleveland Hills, CM=Cumbrian Mountains, FC=Firth of Clyde, FoB=Forest of Bowland, FoF = Firth of Forth, Gr=Grampians, HF =Howgill Fells, LD=Lake District, L=Lewis, M=The Minch, MF=Moray Firth, MV=Midland Valley, NC=North Channel, OH=Outer Hebrides, P=Pennines, Pb=Pembrokeshire, PD=Peak District, YD=Yorkshire Dales. Locations of Figs. 5 and 6 are also shown. Area of the Irish Ice Sheet as considered by Greenwood and Clark (2008ab) shown in grey. In this and subsequent figures, background elevation shading based on NEXTMap Britain (Intermap Technologies, obtained under licence from British Geological Survey ©NERC) and Shuttle Radar Topographic Mission data. Bathymetric contours generated from GEBCO One Minute Grid (GEBCO Digital Atlas published by the British Oceanography Data Centre on behalf of IOC and IHO, 2003).

Figure 2 Illustration of lineation *flowset* derivation from landform mapping: a) extract from Glacial Map of Britain (Hughes *et al.* 2010); b) summarised flow patterns from the subglacial-bedform record; c) grouping of flow patterns based on landform proximity, orientation and parallel conformity; d) resulting *flowsets*.

Figure 3 *Flowsets* of the last British Ice Sheet. Colours indicate classification class (see key). Inset map shows summary ribbed moraine flow patterns (colours here are arbitrary), derived by drawing flow lines perpendicular to ridges and outlines around the spatial extent. Larger (ISO A2 size) version of the map is available as online supplementary material (Fig. S1).

Figure 4 Ancillary evidence used in reconstruction of ice-sheet flow-pattern geometries: a) Retreat pattern map (black) (Clark *et al.* 2012). Outline of the Loch Lomond (Younger Dryas) Stadial ice cap (white) (taken from Clark *et al.* 2004); b) Inferred erratic transport paths (modified from BRITICE database (Clark *et al.* 2004) (Hughes, 2009)); c) British-Irish dates database (Hughes *et al.* 2011; v.2).

Figure 5 Example regional reconstruction for northeast England-Scottish border region. Four flow-pattern geometries are derived from the evidence (left panel: *flowsets* = black, erratic-transport paths = white, retreat pattern = grey): (1) large-scale west-east ice flow places the ice divide to the west, (2) subsequent broadly north-south ice flow along the present-day coastline necessitates an ice divide to the north, (3) topographically-constrained ice flow develops in the Tweed Basin suggesting a thinner ice sheet and ice divides placed over high ground and finally (4) during retreat topographically constrained lobes encircle the high ground of the Cheviots placing an ice divide over or north of the Tweed Basin. We infer cold based ice over the Cheviots, which is supported by the limited spatial expression of Cheviot granite erratics.

Figure 6 Example regional reconstruction for north Scotland. Top panel shows *flowsets* (black), erratic-transport paths (white), shelly-till locations (spotted) and retreat pattern (grey). Below is a sequence of 6 reconstructed ice-sheet geometries that observe the relative-age chronology: (1) NNE ice flow over most of northern Scotland placing an ice divide along Highlands and Grampians. Spatial extent of *flowsets* suggests relatively extensive ice sheet with an offshore margin (three possible margin positions are shown); (2) Major NNW ice flow over North Scotland and Orkney. Highland ice divide has been pushed south; (3) Switch to W-E ice flow over NE Scotland and Orkney indicating reestablishment of Highland ice divide; (4) Ice divide moves east but configuration remains broadly the same; (5) and (6) retreat towards Highlands and Grampians.

1117
1118
1119
1120
1121
1122
1123
1124
1125
1126
1127
1128
1129
1130
1131
1132
1133
1134
1135
1136
1137
1138
1139
1140
1141
1142
1143
1144
1145
1146
1147
1148
1149
1150

Figure 7 Components of the synthesis process to aid grouping of regional reconstructions. Grouping *flowsets* by size and relationship to topography i.e. unconstrained (a) or constrained (b) suggests that the topographically constrained *flowsets* relate to later stages in the ice-sheet evolution (topographically unconstrained *flowsets* are typically the youngest in each region, and vice versa; topographically unconstrained flowsets are larger); (c) The retreat pattern can assist in identification of additional flow patterns related to the deglacial stages of the ice sheet. Panel shows flowsets that correspond to the reconstructed retreat pattern (black); (d) Ice-stream flowsets cross-cut and therefore cannot be organised into a single ice-flow configuration. *Flowset* colour in (a), (b) and (c) is the same as in Fig. 3: TT retreat = green, isochronous = red, TT flowline = blue, TT thinning /thickening = orange.

Figure 8 Model of flow-pattern evolution of the last British Ice Sheet based on palaeoglaciological inversion of the glacial-landform record. Evolution in ice-sheet geometry is presented as a time-series of snapshots that capture significant changes in flow patterns. Ice sheet extent after and including Stage 5 is derived from the reconstructed retreat pattern (Clark *et al.* 2012). Divide/saddle locations and flow patterns are depicted as thick and thin lines respectively. Flowset groupings which form the basis for each snapshot are shown in the background. Colour refers to flowset classification as in Fig. 3. Note that some of the stages are regarded as time-transgressive. White circles mark final retreat locations whose size is below the resolution of the maps. Dotted lines in Stage 7 show estimated extent of remnant ice mass in the southern North Sea and grey lines in Stage 8 show flow pattern necessary to account for ice presence along the eastern English coastline at c. 17 ka BP (see Clark *et al.* 2012). ScIS = Scandinavian Ice Sheet.

Figure 9 Conceptual schematic of bi-modal configurations for an ice sheet resting on an island landmass: a) hypothetical cross profiles of the two modal ice-surface states; b) plan view of the basal topography (contours as indicated) and flow geometries during each state. Note that ~75% of the bed experiences cross-cutting flow patterns and therefore has the potential to preserve superimposed bedforms. At maximum extent the ice extends to the edge of the continental shelf creating extensive marine-terminating margins. When snow accumulation exceeds ice loss by surface melting and iceberg calving (positive mass balance) the ice surface grows yielding a thick ice sheet where divide location and flow geometry are largely independent of topography (i.e. an ice sheet *sensu stricto*) (1). With a negative mass balance, the ice sheet thins and the flow geometry is increasingly influenced by basal topography; ice divides eventually becoming anchored to major upland areas (creating a complex of ice caps) (2).

Figure 1
[Click here to download high resolution image](#)

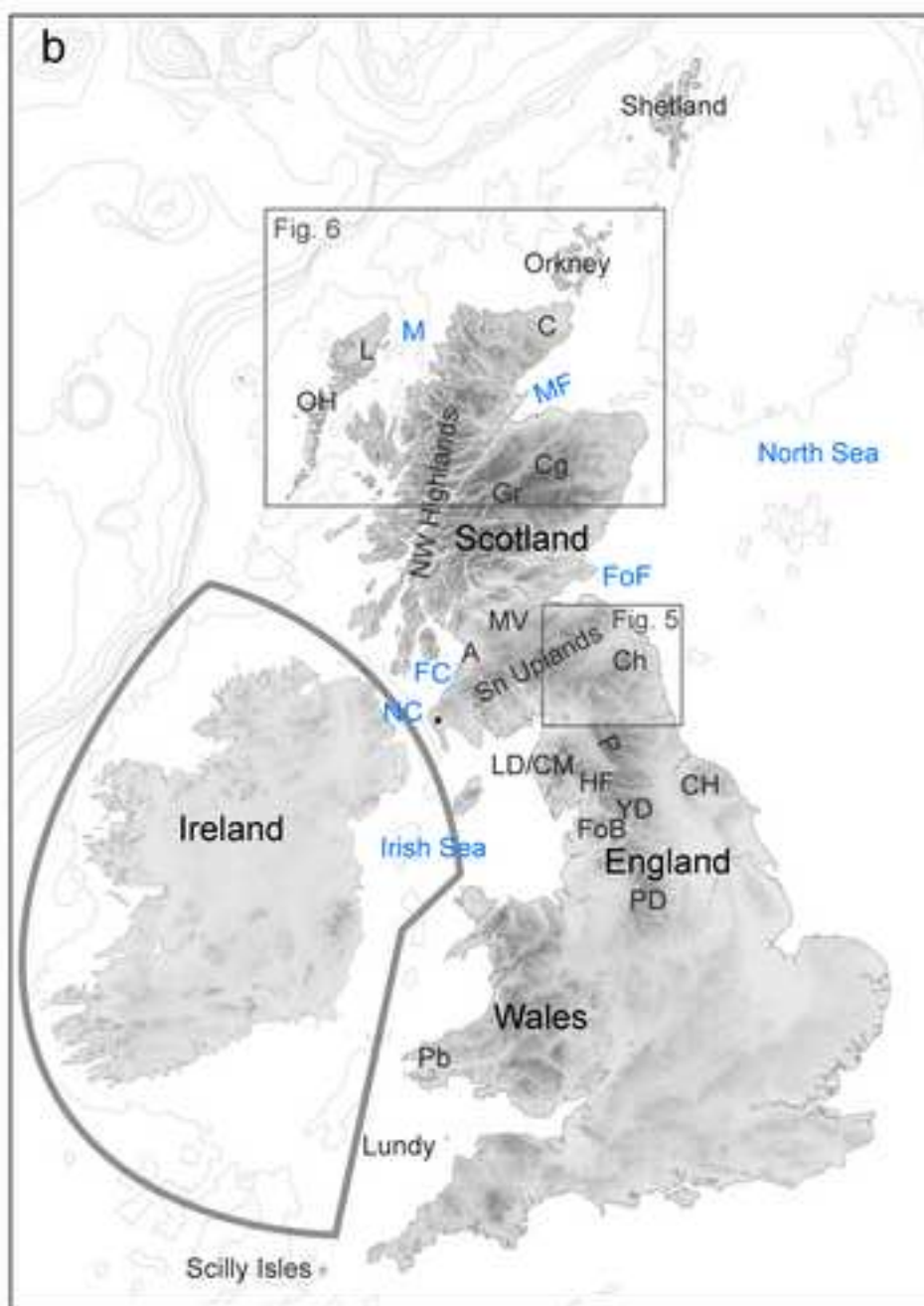


Figure 2
[Click here to download high resolution image](#)

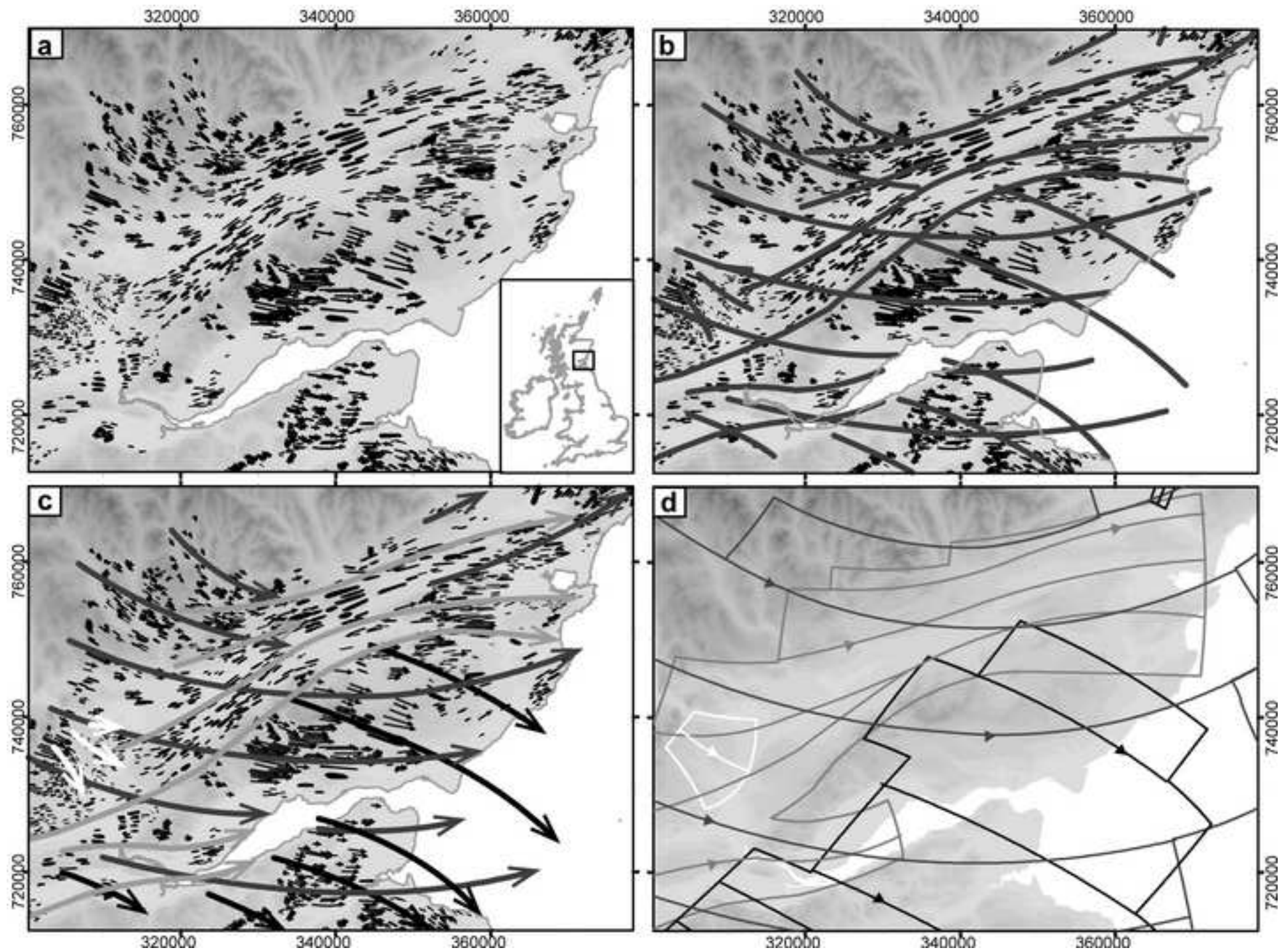


Figure 3
[Click here to download high resolution image](#)

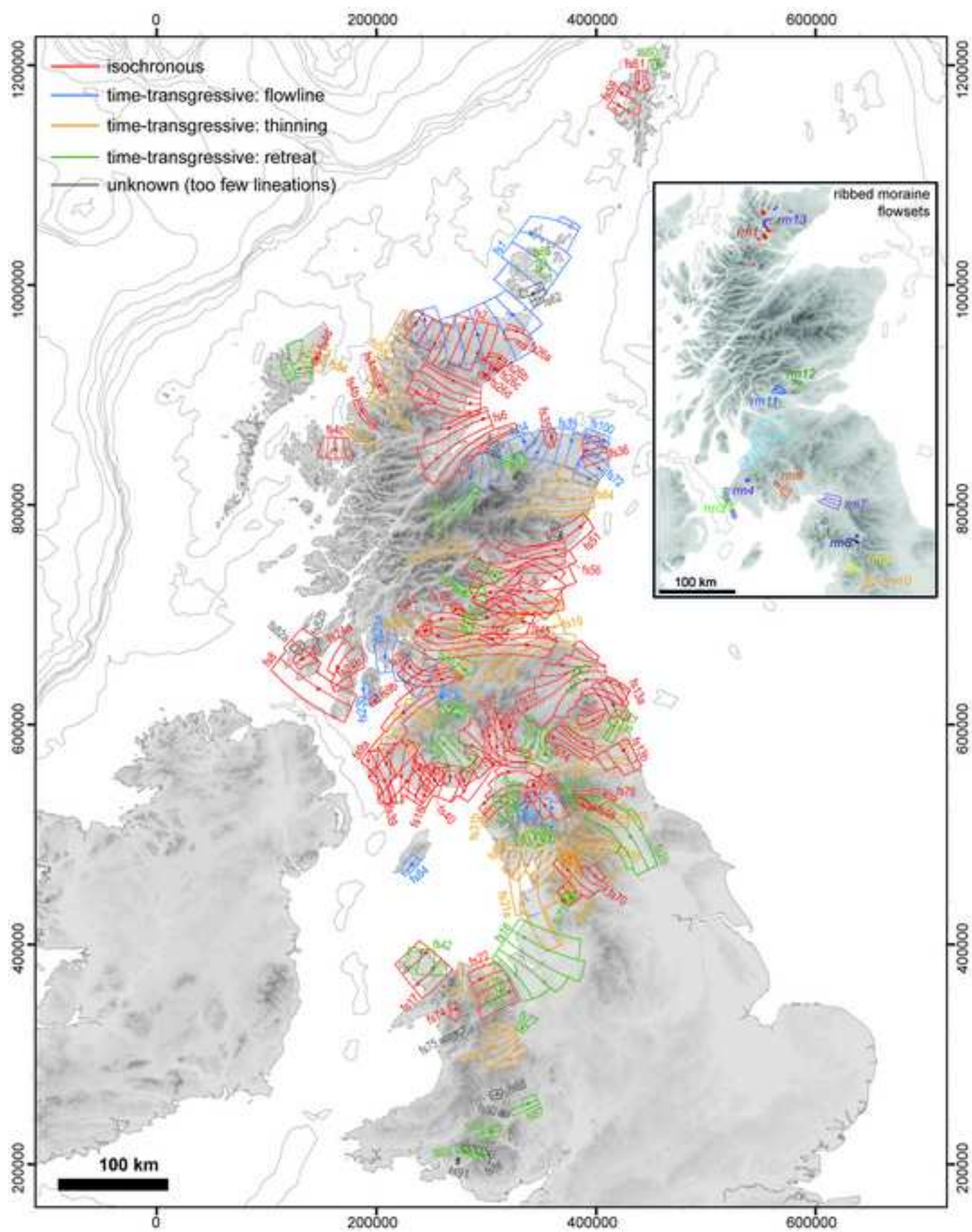


Figure 4
[Click here to download high resolution image](#)

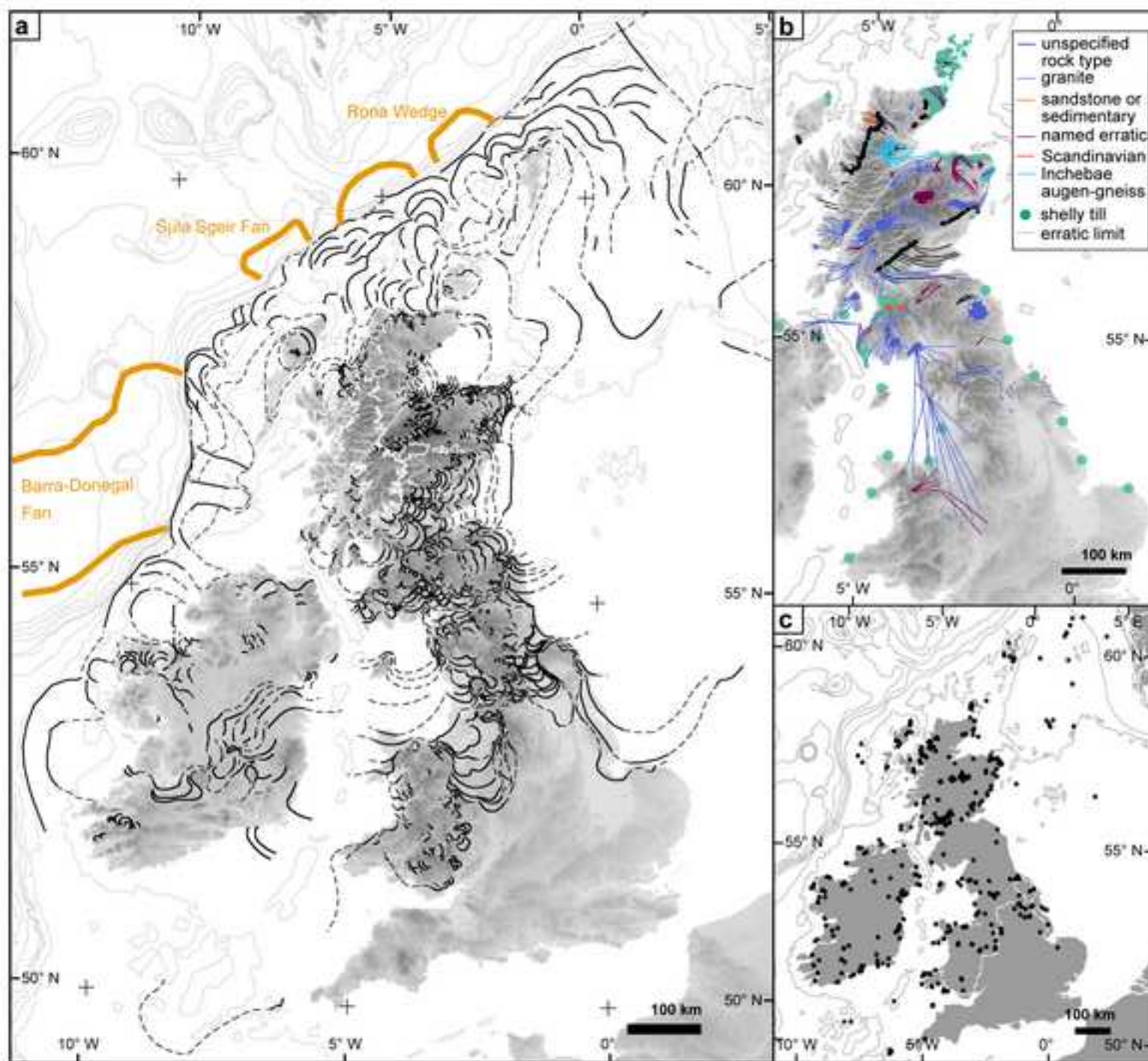


Figure 5
[Click here to download high resolution image](#)

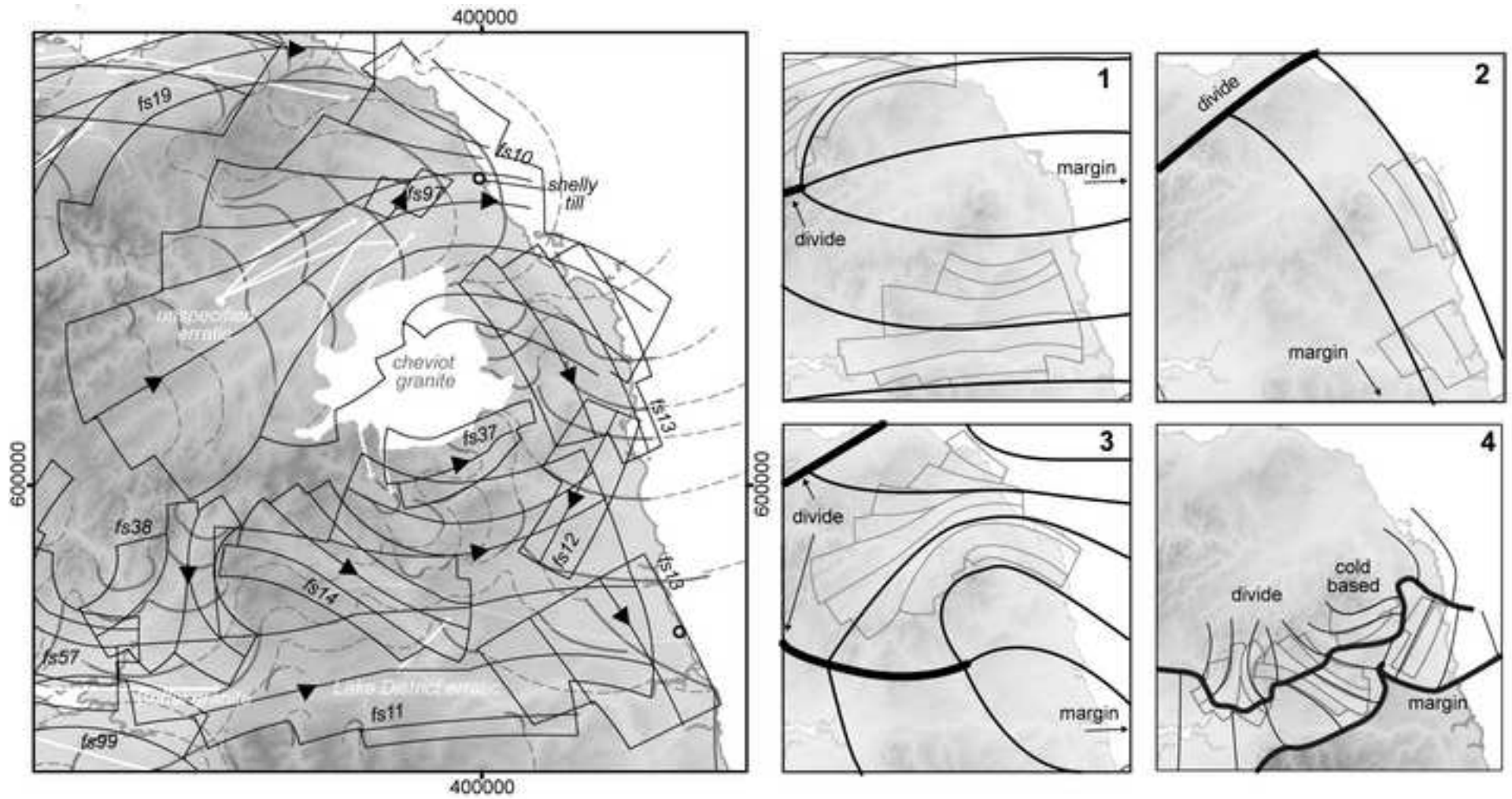


Figure 6
[Click here to download high resolution image](#)

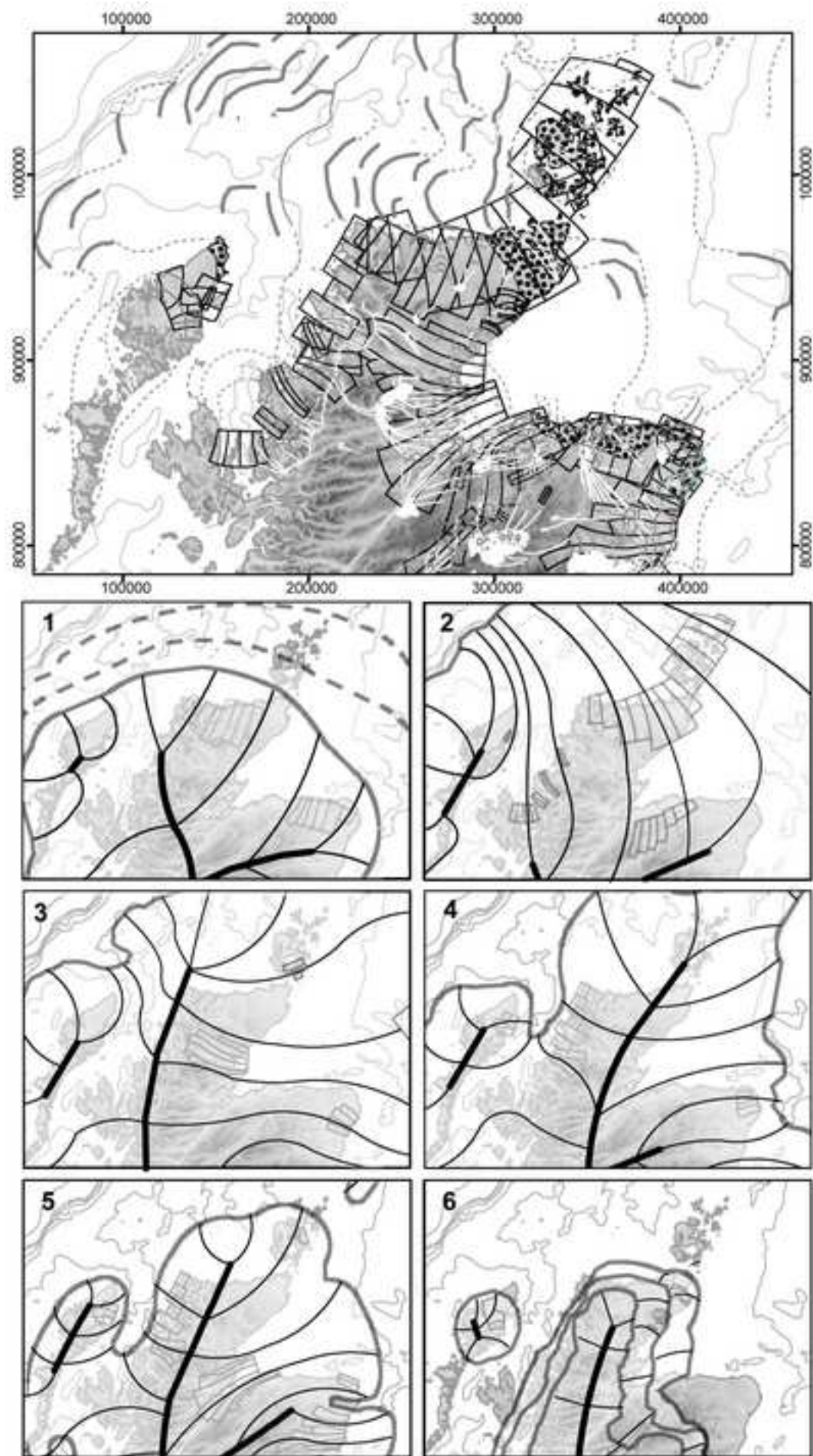


Figure 7
[Click here to download high resolution image](#)

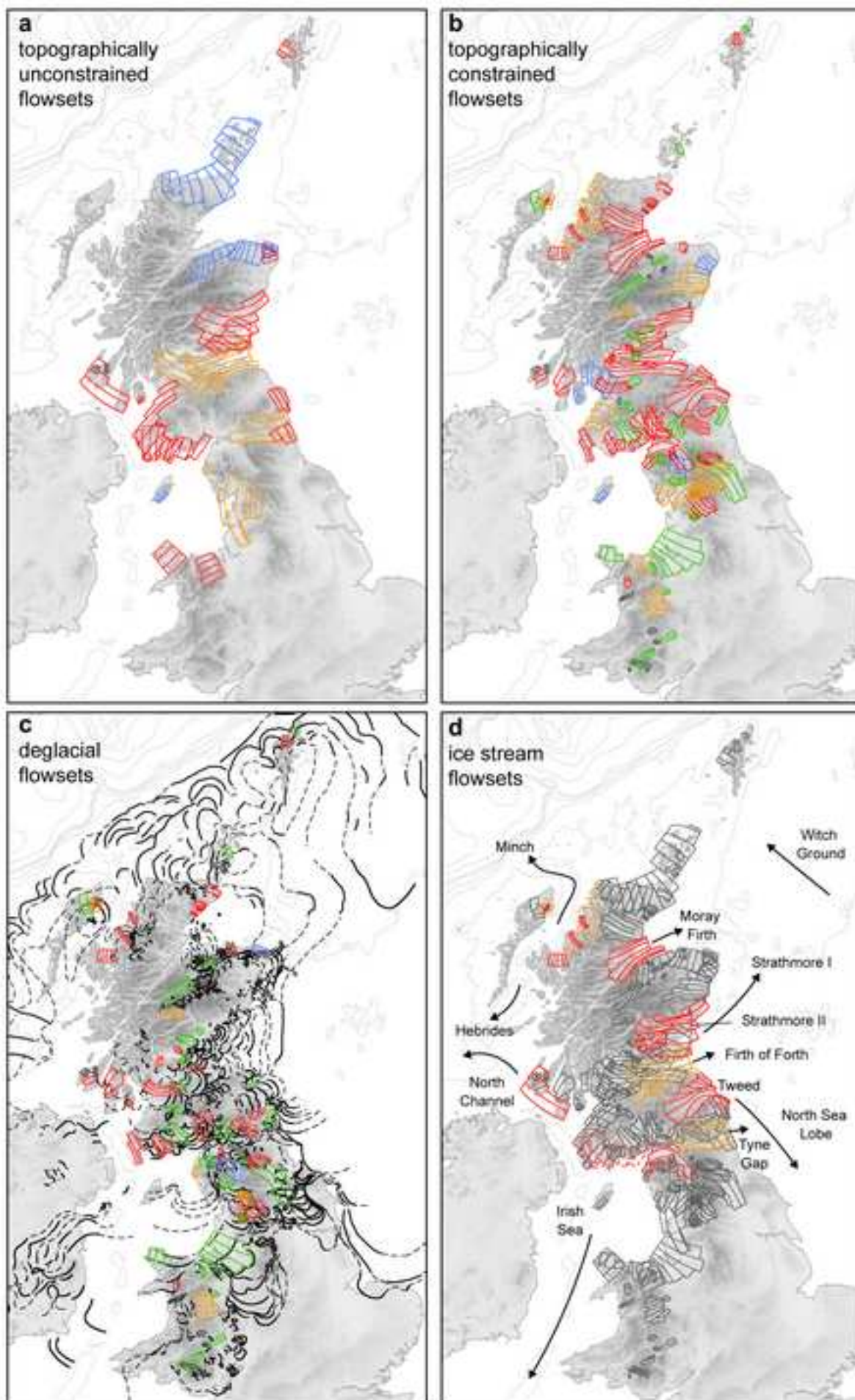


Figure 8
[Click here to download high resolution image](#)

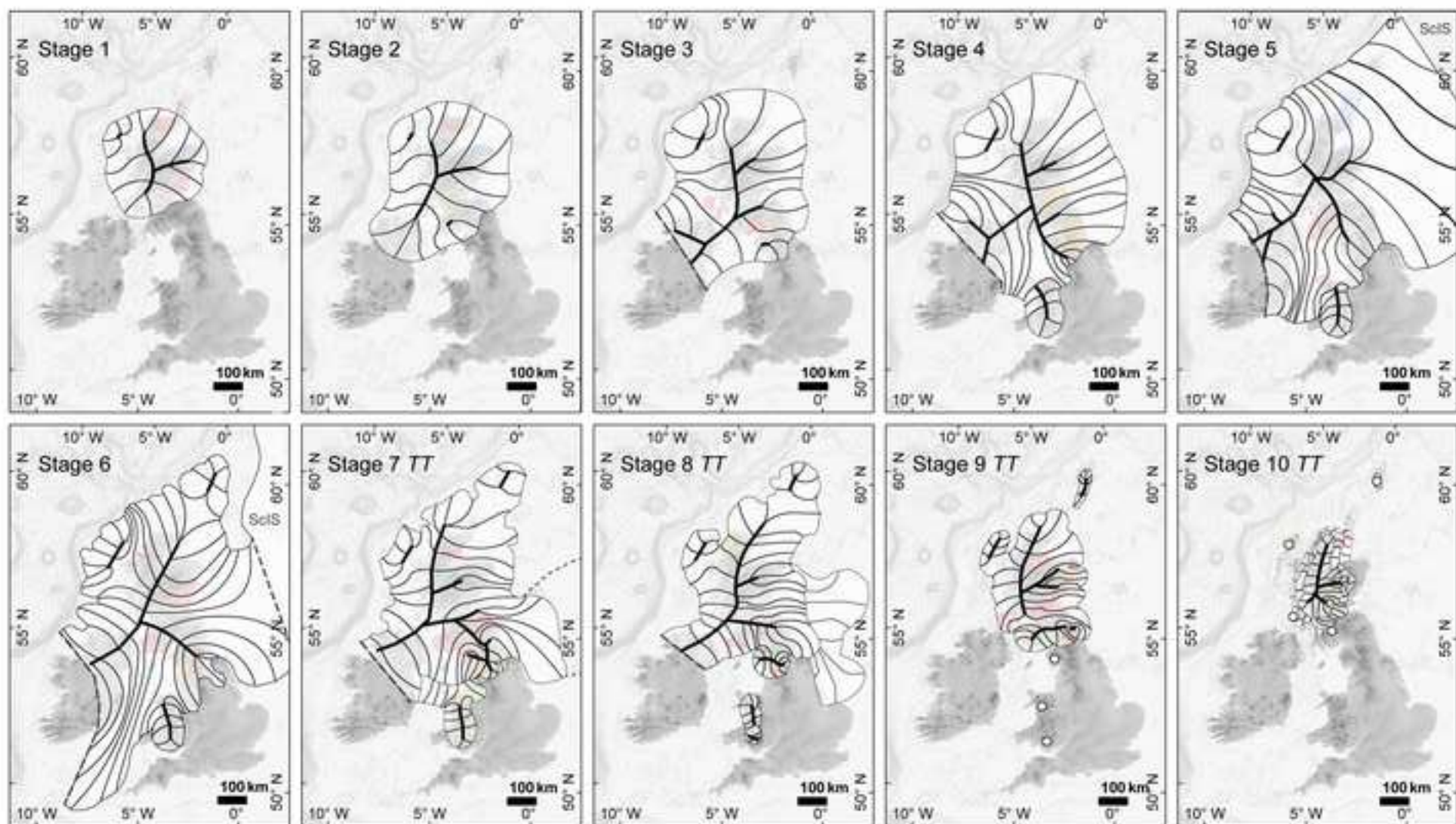
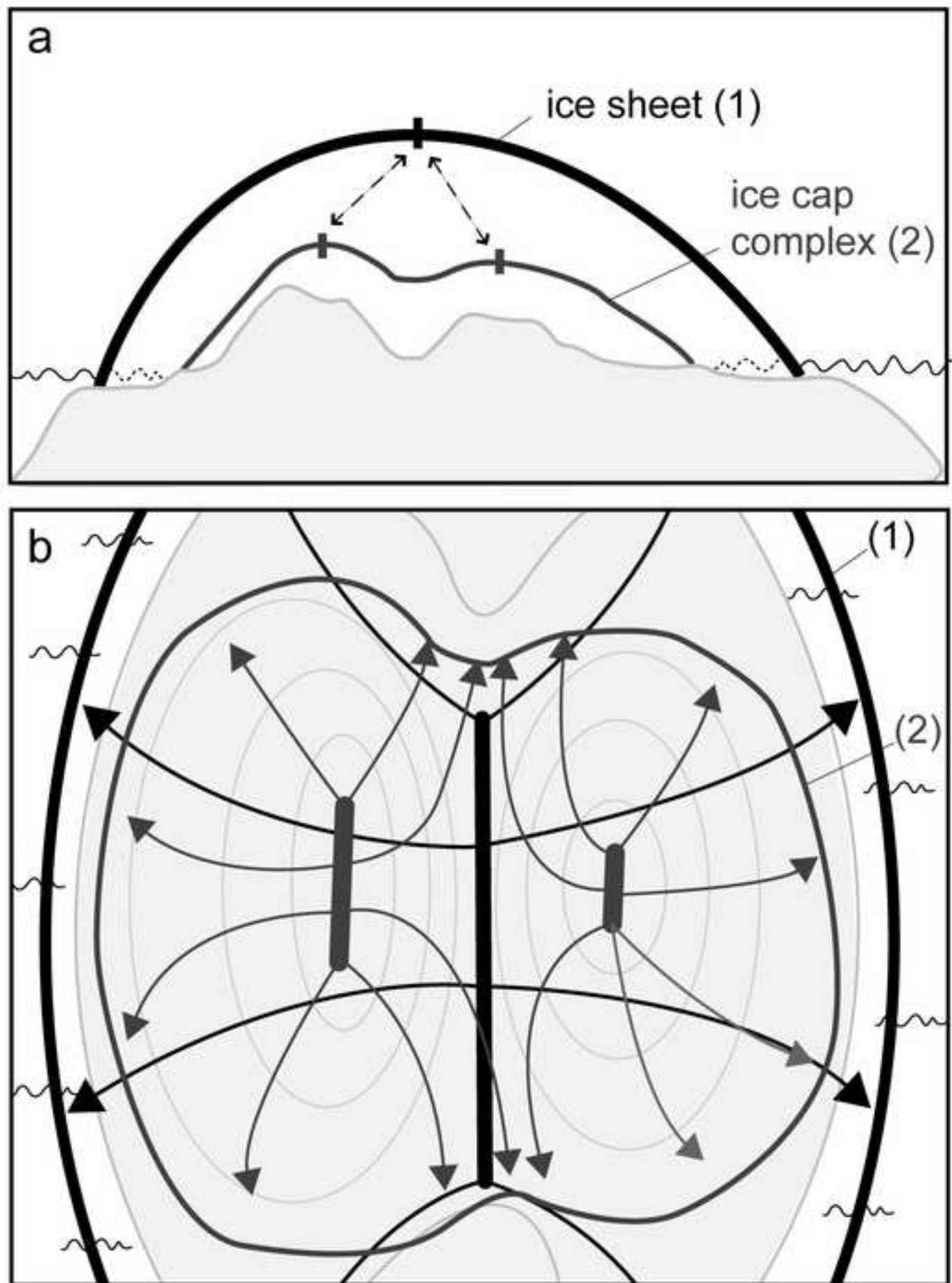


Figure 9
[Click here to download high resolution image](#)



Supplementary Data Figure S1

[Click here to download Supplementary Data: FigS1.pdf](#)

Supplementary Data Table S1

[Click here to download Supplementary Data: TableS1.pdf](#)